

On the two-loop BSM corrections to $h \longrightarrow \gamma\gamma$ in a triplet extension of the SM

Giuseppe Degrassi^a and Pietro Slavich^b

^a *Dipartimento di Matematica e Fisica, Università di Roma Tre,
and INFN, Sezione di Roma Tre, I-00146 Rome, Italy.*

^b *Sorbonne Université, CNRS, Laboratoire de Physique Théorique et Hautes Energies,
LPTHE, F-75005, Paris, France.*

Abstract

We compute the two-loop BSM contributions to the $h \longrightarrow \gamma\gamma$ decay width in the SM extended with a real triplet of $SU(2)$. We consider scenarios in which the neutral components of doublet and triplet do not mix, so that the lighter neutral scalar h has (at least approximately) SM-like couplings to fermions and gauge bosons. We focus on the two-loop corrections controlled by the quartic scalar couplings, and obtain explicit and compact formulas for the $h\gamma\gamma$ amplitude by means of a low-energy theorem that connects it to the derivative of the photon self-energy w.r.t. the Higgs field. We briefly discuss the numerical impact of the newly-computed contributions, showing that they may be required for a precise determination of $\Gamma[h \rightarrow \gamma\gamma]$ in scenarios where the quartic scalar couplings are large.

1 Introduction

The discovery of a Higgs boson with mass around 125 GeV [1, 2] and properties compatible with the predictions of the Standard Model (SM) [3] goes a long way towards elucidating the mechanism of electroweak (EW) symmetry breaking, but does not by itself preclude the existence of additional Higgs bosons with masses around or even below the TeV scale, which could still be discovered in the current or future runs of the LHC. Apart from the requirement that they allow for a 125-GeV scalar with SM-like couplings to fermions and gauge bosons, the parameters of beyond-the-SM (BSM) models with an extended Higgs sector are subject to a number of experimental constraints from direct searches for new particles, EW precision observables, and flavor physics, as well as theory-driven constraints from perturbative unitarity, perturbativity, and the stability of the scalar potential. However, it is often found that, in BSM models, some of the quartic Higgs couplings can be of $\mathcal{O}(1-10)$ without violating any of the above-mentioned constraints. This applies in particular to “bottom-up” constructions in which the extended Higgs sector is not embedded in a supersymmetric model supposed to be valid up to scales much higher than the TeV. Couplings in this range may induce sizable radiative corrections to the predictions for physical observables, up to the point where one might wonder whether, in any given calculation, the uncomputed higher-order effects spoil the accuracy of the prediction.

In the Two-Higgs-Doublet Model (THDM) [4–6], one of the simplest and best-studied extensions of the SM, the viability of scenarios with large quartic Higgs couplings motivated a number of recent studies in which radiative corrections involving those couplings were computed at the two-loop level. In particular, the two-loop corrections to the ρ parameter were computed in refs. [7,8], various effects of the two-loop corrections to the scalar mass matrices were examined in ref. [9], the two-loop corrections to the trilinear self-coupling of the SM-like Higgs boson, λ_{hhh} , were computed in refs. [10,11], and the two-loop corrections to the decay width for the process $h \rightarrow \gamma\gamma$ were computed in refs. [12,13]. In all cases it was found that the two-loop corrections can significantly modify the one-loop predictions, and should be taken into account for a precise determination of the considered observable.

In this paper we consider an extension of the SM, which we refer to as the TSM, where the Higgs sector is augmented with a real ($Y = 0$) triplet of $SU(2)$, so that the spectrum of physical Higgs states includes two neutral scalars, h and H , and a charged scalar, H^\pm . The model was first introduced in ref. [14], and the contributions of the triplet to the EW precision observables were computed in refs. [15–23], where different ways to connect the parameters of the TSM to a set of physical inputs were extensively discussed. Various aspects of the phenomenology of the TSM at the LHC were explored in refs. [24–32], and the possibility that the recent measurement of the W boson mass by CDF [33], which is 7σ away from the SM prediction¹, is accommodated in the TSM through a small vacuum expectation value (vev) for the triplet was discussed, e.g., in refs. [36,37].

Any realistic extension of the SM must be able to accommodate the measured – and essentially SM-like – properties of the Higgs boson already discovered at the LHC. Among those properties, the width for the loop-induced decay $h \rightarrow \gamma\gamma$ plays a special role, because the corresponding signal

¹Note that more-recent measurements of m_W by ATLAS [34] and CMS [35] are within 1σ from the SM prediction.

strength is already measured with an accuracy of about 6% [3], bound to further improve as more data are collected at the LHC, and because both SM and BSM particles contribute to it at the leading order (LO), i.e., at the one-loop level. Indeed, most of the phenomenological analyses of the TSM in refs. [24–32] considered the constraints on the model’s parameter space that arise from the LO prediction for $\Gamma(h \rightarrow \gamma\gamma)$, which receives a BSM contribution from one-loop diagrams involving the charged scalar H^\pm . In this paper we take one step beyond the LO, and compute the BSM contributions to $\Gamma(h \rightarrow \gamma\gamma)$ from two-loop diagrams controlled by the scalar couplings involving the triplet, which, as mentioned earlier, can in principle be of $\mathcal{O}(1-10)$. We closely follow our approach from ref. [12], where an analogous calculation was performed for the THDM. In particular, we consider only “aligned” scenarios in which the neutral components of doublet and triplet do not mix, so that the lighter neutral scalar h , which we assume to be part of the doublet, has (at least approximately) SM-like couplings to fermions and gauge bosons. The choice of focusing on the effects of the potentially-large scalar couplings that involve the triplet allows us to neglect the contributions of two-loop diagrams involving the gauge and Yukawa couplings (except of course for the electromagnetic couplings of the external photons), and to neglect the mass of the SM-like Higgs boson w.r.t. the masses of the triplet-like states. In this case, we can exploit a low-energy theorem (LET) that connects the $h\gamma\gamma$ amplitude to the derivative of the photon self-energy w.r.t. the vev of the SM-like Higgs field [38, 39], but we also cross-check our results via a direct calculation of the amplitude.

The rest of the article is organized as follows: in section 2 we fix our notation for the Higgs sector of the TSM and introduce two distinct scenarios in which the neutral components of doublet and triplet do not mix; in section 3 we outline our calculation of the dominant two-loop corrections to the decay width for $h \rightarrow \gamma\gamma$ in the two considered scenarios; in section 4 we briefly discuss the numerical impact of the newly-computed corrections; section 5 contains our conclusions; finally, three appendices collect explicit formulas for the one-loop self-energies and tadpoles that are relevant to our calculation, for the two-loop BSM contribution to the $h\gamma\gamma$ amplitude, and for the Higgs-mass dependence of the $h\gamma\gamma$ amplitude at one loop.

2 The Higgs sector of the TSM

In this section we describe the Higgs sector of the TSM at the tree level. The scalar potential of the SM extended with an $SU(2)$ triplet with $Y = 0$ can be parametrized as²

$$\begin{aligned}
V_0 = & \mu^2 H^\dagger H + \frac{m_T^2}{2} \text{Tr}(T^2) + \frac{\lambda_H}{2} (H^\dagger H)^2 + \frac{\lambda_T}{2} \text{Tr}(T^4) \\
& + \kappa_{HT} H^\dagger T H + \frac{\lambda_{HT}}{2} H^\dagger H \text{Tr}(T^2) ,
\end{aligned} \tag{1}$$

²We employ the same conventions as in the “SM+Triplet-Real” model file implemented in the code SARAH [40–44]. For comparison, the conventions of ref. [27] correspond to the replacements $\mu^2 \rightarrow -\mu_H^2$, $m_T^2 \rightarrow -\mu_\Sigma^2$, $\lambda_H \rightarrow 2\lambda_H$, $\lambda_T \rightarrow b_4$, $\kappa_{HT} \rightarrow a_1/\sqrt{2}$, $\lambda_{HT} \rightarrow a_2$, $v \rightarrow v_H$, $v_T \rightarrow \sqrt{2}v_\Sigma$. For an early discussion of the tree-level scalar potential and mass spectrum of the TSM, see ref. [45].

where H is the SM-like Higgs doublet and T is the triplet. The scalar potential in eq. (1) is bounded from below if $\lambda_H > 0$, $\lambda_T > 0$ and $\lambda_{HT} > -\sqrt{2\lambda_H\lambda_T}$. Expanded around their vevs v and v_T , respectively, the doublet and triplet fields can be decomposed as

$$H = \frac{1}{\sqrt{2}} \begin{pmatrix} \sqrt{2}\phi_H^+ \\ v + \phi_H^0 + iG^0 \end{pmatrix}, \quad T = \frac{1}{\sqrt{2}} \begin{pmatrix} \frac{v_T}{\sqrt{2}} + \phi_T^0 & \sqrt{2}\phi_T^+ \\ \sqrt{2}\phi_T^- & -\frac{v_T}{\sqrt{2}} - \phi_T^0 \end{pmatrix}. \quad (2)$$

The tree-level tadpoles for the doublet and the triplet, respectively, are

$$\tau_H \equiv \left. \frac{\partial V_0}{\partial \phi_H^0} \right|_{\min} = v \left(\mu^2 + \frac{\lambda_H}{2} v^2 + \frac{\lambda_{HT}}{4} v_T^2 - \frac{\kappa_{HT}}{2} v_T \right), \quad (3)$$

$$\tau_T \equiv \left. \frac{\partial V_0}{\partial \phi_T^0} \right|_{\min} = \frac{v_T}{\sqrt{2}} \left(m_T^2 + \frac{\lambda_T}{2} v_T^2 + \frac{\lambda_{HT}}{2} v^2 - \frac{\kappa_{HT}}{2} \frac{v^2}{v_T} \right). \quad (4)$$

The tree-level minimum conditions for the scalar potential correspond to $\tau_H = \tau_T = 0$, and a realistic EWSB scenario requires $v \neq 0$. As discussed, e.g., in ref. [24], when $\kappa_{HT} = 0$ the only realistic solution of the minimum conditions leads to $v^2 = -2\mu^2/\lambda_H$ and $v_T = 0$ (another possible solution where both v and v_T are different from zero involves a massless physical scalar). Conversely, eq. (4) shows that $\kappa_{HT} \neq 0$ implies in turn $v_T \neq 0$. In the latter case, the minimum conditions can be exploited to express both of the mass parameters μ^2 and m_T^2 as combinations of the other Lagrangian parameters and the vevs. The tree-level mass matrices \mathcal{M}_0^2 and \mathcal{M}_\pm^2 for the neutral scalars (ϕ_H^0, ϕ_T^0) and the charged scalars (ϕ_H^\pm, ϕ_T^\pm), respectively, can thus be written as

$$\mathcal{M}_0^2 = \begin{pmatrix} \lambda_H v^2 & \frac{v}{\sqrt{2}} (\lambda_{HT} v_T - \kappa_{HT}) \\ \frac{v}{\sqrt{2}} (\lambda_{HT} v_T - \kappa_{HT}) & \lambda_T v_T^2 + \frac{\kappa_{HT}}{2} \frac{v^2}{v_T} \end{pmatrix}, \quad (5)$$

$$\mathcal{M}_\pm^2 = \begin{pmatrix} \kappa_{HT} v_T & \frac{\kappa_{HT}}{\sqrt{2}} v \\ \frac{\kappa_{HT}}{\sqrt{2}} v & \frac{\kappa_{HT}}{2} \frac{v^2}{v_T} \end{pmatrix}. \quad (6)$$

The mass eigenstates are obtained via rotations by the angles³ γ and δ :

$$\begin{pmatrix} h \\ H \end{pmatrix} = \begin{pmatrix} c_\gamma & s_\gamma \\ -s_\gamma & c_\gamma \end{pmatrix} \begin{pmatrix} \phi_H^0 \\ \phi_T^0 \end{pmatrix}, \quad \begin{pmatrix} G^\pm \\ H^\pm \end{pmatrix} = \begin{pmatrix} c_\delta & s_\delta \\ -s_\delta & c_\delta \end{pmatrix} \begin{pmatrix} \phi_H^\pm \\ \phi_T^\pm \end{pmatrix}. \quad (7)$$

In particular, for the charged scalars one finds

$$\delta = -\arctan\left(\frac{\sqrt{2}v_T}{v}\right), \quad m_{G^\pm}^2 = 0, \quad m_{H^\pm}^2 = \kappa_{HT} v_T \left(1 + \frac{v^2}{2v_T^2}\right). \quad (8)$$

Finally, the tree-level masses for the gauge bosons and the tree-level Fermi constant are

$$m_Z^2 = \frac{g^2 + g'^2}{4} v^2, \quad m_W^2 = \frac{g^2}{4} (v^2 + 2v_T^2) = \frac{g^2}{4} v^2 c_\delta^{-2}, \quad (\sqrt{2}G_\mu)^{-1} = (v^2 + 2v_T^2)^{-1/2} = v^2 c_\delta^{-2}, \quad (9)$$

³We will henceforth use the shortcuts $c_\theta \equiv \cos \theta$, $s_\theta \equiv \sin \theta$, and $t_\theta \equiv \tan \theta$ for a generic angle θ .

where g and g' are the $SU(2)$ and $U(1)$ gauge couplings, respectively. We recall here that the usual approach to the analysis of the EW sector of the SM consists in treating m_Z , G_μ , and $\alpha_{\text{em}} \equiv e^2/(4\pi)$, where e is the electric charge, as physical input quantities, and obtaining predictions for m_W^2 and for $\theta_W \equiv \arctan(g'/g)$. In extensions of the SM we can write:

$$m_W^2 = \frac{1}{2} m_Z^2 \rho \left(1 + \sqrt{1 - \frac{2\sqrt{2}\pi\alpha_{\text{em}}}{G_\mu m_Z^2 \rho}} \right), \quad s_{\theta_W}^2 = \frac{1}{2} \left(1 - \sqrt{1 - \frac{2\sqrt{2}\pi\alpha_{\text{em}}}{G_\mu m_Z^2 \rho}} \right), \quad (10)$$

where $\rho \equiv m_W^2/(m_Z^2 c_{\theta_W}^2)$ is treated as an additional input parameter. In the SM $\rho = 1$ at the tree level, but in the TSM the presence of a (small) vev for the triplet leads to $\rho \gtrsim 1$. As discussed, e.g., in ref. [46], this causes shifts in both m_W^2 and θ_W w.r.t. the corresponding SM predictions. Expanding eq. (10) in $\Delta\rho \equiv \rho - 1$, we get:

$$\Delta m_W^2 \approx \frac{c_{\theta_W}^2}{c_{\theta_W}^2 - s_{\theta_W}^2} m_W^2 \Delta\rho, \quad \Delta s_{\theta_W}^2 \approx -\frac{c_{\theta_W}^2 s_{\theta_W}^2}{c_{\theta_W}^2 - s_{\theta_W}^2} \Delta\rho. \quad (11)$$

Eq. (9) shows that in the TSM $\rho = c_\delta^{-2}$ at the tree level, hence $\Delta\rho = t_\delta^2 = 2v_T^2/v^2$. Reconciling the SM prediction $m_W^{\text{SM}} = 80.356$ GeV [3] with the CDF measurement $m_W^{\text{CDF}} = 80.433$ GeV [33] would require $v_T \approx 6.4$ GeV.⁴

In our calculation of the diphoton decay width of the SM-like Higgs boson we will focus on scenarios in which the neutral components of doublet and triplet do not mix, i.e., $\gamma = 0$. According to eq. (5), this can be realized when $\kappa_{HT} = \lambda_{HT} v_T$, in which case the minimum condition $\tau_T = 0$ implies $m_T^2 = -\lambda_T v_T^2/2$, see eq. (4), and the tree-level masses of the physical states can be written as

$$m_h^2 = \lambda_H v^2, \quad m_H^2 = \frac{\lambda_{HT}}{2} v^2 + \lambda_T v_T^2, \quad m_{H^\pm}^2 = \frac{\lambda_{HT}}{2} v^2 \left(1 + \frac{2v_T^2}{v^2} \right). \quad (12)$$

In view of the small value of v_T , the neutral and charged triplet-like states are almost degenerate in mass. This scenario – which we will call “**scenario A**” in the following – is called “fermiophobic” in ref. [30] because the neutral component of the triplet, H , does not couple to fermions and can have sizeable branching ratios to pairs of W bosons or photons (in contrast, H^\pm can still decay to fermion pairs through its small doublet component). The neutral component of the doublet, h , has approximately SM-like couplings to fermions and gauge bosons at the tree level. In fact, the couplings of h to fermion pairs and to Z -boson pairs are enhanced by c_δ^{-1} w.r.t. the corresponding SM predictions expressed as combinations of masses and G_μ , and the couplings of h to W -boson pairs are suppressed by c_δ , but even the relatively large value $v_T \approx 6.4$ GeV, which could be considered as an upper bound of the acceptable range for the triplet vev, corresponds to $c_\delta \approx 0.999$.

⁴Neglecting the effect of the triplet vev on the prediction for θ_W , as done, e.g., in refs. [29, 36, 37], one would instead find $\Delta m_W^2 \approx m_W^2 \Delta\rho$, and the CDF result would imply $v_T \approx 7.6$ GeV with our normalization of the vev.

A different scenario in which the neutral doublet-like and triplet-like states do not mix – which we will call “**scenario B**” in the following – is realized when $\kappa_{HT} = v_T = 0$, in which case the scalar potential possesses a discrete Z_2 symmetry for $T \rightarrow -T$ that forbids the mixing. In this scenario eq. (4) cannot be used to replace m_T^2 with a combination of the other Lagrangian parameters and the vevs, and the tree-level masses of the physical states can be written as

$$m_h^2 = \lambda_H v^2, \quad m_H^2 = m_{H^\pm}^2 = m_T^2 + \frac{\lambda_{HT}}{2} v^2. \quad (13)$$

The requirement that the SM-like minimum of the scalar potential be deeper than an unphysical minimum with $v = 0$ and $v_T \neq 0$ implies $m_T^2 > -\sqrt{\lambda_T/2} m_h v$. When the triplet mass is treated as an input parameter instead of m_T^2 , this translates to $\lambda_{HT} < 2(m_{H^\pm}^2 + \sqrt{\lambda_T/2} m_h v)/v^2$. We remark that the mass spectra of the scenarios A and B coincide when the limit $v_T \rightarrow 0$ is taken in eq. (12) and the limit $m_T^2 \rightarrow 0$ is taken in eq. (13).

The degeneracy of the tree-level masses of the triplet-like states in the scenario B is lifted by small radiative corrections involving the EW gauge bosons, so that $m_{H^\pm} \gtrsim m_H$. The neutral component of the triplet, H , is stable and can serve as a Dark Matter (DM) candidate [47], while the neutral component of the doublet, h , has exactly SM-like couplings to fermions and to gauge bosons at the tree level. The charged scalar H^\pm decays to $H\pi^\pm$, $He^\pm\nu_e$ or $H\mu^\pm\nu_\mu$, giving rise to a disappearing track at the LHC because the charged particle in the final state is too soft to be detected. The interplay between the constraints on this scenario from DM searches and from direct searches at the LHC was discussed in refs. [24, 27, 28].

While the measured value of the Higgs mass determines the quartic self-coupling of the doublet to be $\lambda_H \approx 0.26$ when $\gamma = 0$, the quartic couplings that involve the triplet, λ_{HT} and λ_T , are free parameters of the TSM, bounded from above only by theoretical considerations. The upper bounds from tree-level perturbative unitarity (i.e., the requirement that the tree-level $2 \rightarrow 2$ scattering amplitudes remain unitary at high energies) were discussed, e.g., in refs. [26, 27, 48], and amount to $\lambda_{HT} \lesssim 14$ and $\lambda_T \lesssim 5$. The upper bounds from perturbativity (i.e., the requirement that the couplings themselves are not so large as to spoil the convergence of the perturbative series) involve some degree of subjectivity: for example, some studies in the literature apply upper bounds of 4π [48, 49] or of $2\sqrt{\pi}$ [24, 25, 30] to both couplings, while ref. [27] applies upper bounds derived from the fixed points of the two-loop RGEs,⁵ leading to $\lambda_{HT} \lesssim 8$ and $\lambda_T \lesssim 4$. In any case, it appears that the couplings that involve the triplet can be considerably larger than the SM couplings without violating any of the theoretical bounds. In such scenarios, the radiative corrections controlled by those couplings can be legitimately expected to be the dominant ones.

⁵The bound $\lambda_T \lesssim 2$ quoted in ref. [27] was obtained with an older version of the code `SARAH`, in which the model file “`SM+Triplet-Real`” contained a bug that affected the RGEs.

3 Leading two-loop contributions to $\Gamma[h \rightarrow \gamma\gamma]$

We now discuss our calculation of the dominant two-loop corrections to $\Gamma[h \rightarrow \gamma\gamma]$ in the TSM, in which we closely follow the approach of the THDM calculation of ref. [12]. We consider the two scenarios mentioned earlier, in which the neutral components of the doublet and triplet scalars do not mix, and we focus on the two-loop BSM corrections that are controlled by the potentially large quartic couplings λ_{HT} and λ_T . In contrast, we neglect all corrections involving the gauge and Yukawa couplings. We also treat the mass of the SM-like Higgs boson as negligible w.r.t. the masses of the BSM Higgs bosons, which allows us to use the LET of refs. [38, 39] to connect the $h\gamma\gamma$ amplitude to the derivative of the photon self-energy w.r.t. the doublet vev.

3.1 The LET and the calculation of the photon self-energy

The partial width for the $h \rightarrow \gamma\gamma$ decay can be written as

$$\Gamma(h \rightarrow \gamma\gamma) = \frac{G_\mu \alpha_{\text{em}}^2 M_h^3}{128 \sqrt{2} \pi^3} \left| \mathcal{P}_h^{1\ell} + \mathcal{P}_h^{2\ell} \right|^2, \quad (14)$$

where we recall that the Fermi constant G_μ is proportional to c_δ^2/v^2 at the tree level. $\mathcal{P}_h^{1\ell}$ and $\mathcal{P}_h^{2\ell}$ denote the one- and two-loop $h\gamma\gamma$ amplitudes, respectively. The latter can be further decomposed as

$$\mathcal{P}_h^{2\ell} = \mathcal{P}_h^{2\ell, \text{1PI}} + \Delta\mathcal{P}_h^{1\ell} + \delta\mathcal{P}_h^{1\ell} + K_r \mathcal{P}_h^{1\ell}, \quad (15)$$

where: $\mathcal{P}_h^{2\ell, \text{1PI}}$ denotes the genuine two-loop part, in which we include the one-particle-irreducible (1PI) contributions as well as the $\overline{\text{MS}}$ counterterm contributions; $\Delta\mathcal{P}_h^{1\ell}$ stems from the minimum conditions for the scalar potential, and from the conditions of vanishing SM-like Higgs mass and vanishing mixing between the neutral scalars; $\delta\mathcal{P}_h^{1\ell}$ stems from renormalization-scheme choices for the parameters entering $\mathcal{P}_h^{1\ell}$ (in particular, $\delta\mathcal{P}_h^{1\ell} = 0$ would correspond to all parameters being in the $\overline{\text{MS}}$ scheme); the additional correction factor K_r accounts for the diagonal WFR of the external Higgs field and for the renormalization of G_μ .

In the approximation of vanishing external momentum for the $h\gamma\gamma$ amplitude (i.e., vanishing mass for the SM-like Higgs boson), the LET of refs. [38, 39] allows us to write⁶

$$\mathcal{P}_h^{1\ell} = \frac{2\pi v c_\delta^{-1}}{\alpha_{\text{em}}} \frac{d\Pi_{\gamma\gamma}^{1\ell}(0)}{dv}, \quad \mathcal{P}_h^{2\ell, \text{1PI}} = \frac{2\pi v c_\delta^{-1}}{\alpha_{\text{em}}} \frac{d\Pi_{\gamma\gamma}^{2\ell}(0)}{dv}, \quad (16)$$

where $\Pi_{\gamma\gamma}(0)$ denotes the transverse part of the dimensionless self-energy of the photon at vanishing external momentum. At the one-loop level, it reads

$$\Pi_{\gamma\gamma}^{1\ell}(0) = \Pi_{\gamma\gamma}^{1\ell, H^\pm}(0) + \Pi_{\gamma\gamma}^{1\ell, t}(0) + \Pi_{\gamma\gamma}^{1\ell, W}(0)$$

⁶Compared with the analogous formulas for the THDM, see eq. (39) of ref. [12], the additional factors c_δ^{-1} stem from the different relation between G_μ and v in the TSM.

$$= \frac{\alpha_{\text{em}}}{4\pi} \left(\frac{1}{3} \ln \frac{m_{H^\pm}^2}{Q^2} + \frac{4}{3} Q_t^2 N_c \ln \frac{m_t^2}{Q^2} - 7 \ln \frac{m_W^2}{Q^2} + \frac{2}{3} \right), \quad (17)$$

where Q is the renormalization scale, $N_c = 3$ is a color factor, $Q_t = 2/3$ is the electric charge of the top quark, and we omitted all other fermionic contributions because the corresponding contributions to the $h\gamma\gamma$ amplitude are suppressed by the small fermion masses. The contribution of the gauge sector, $\Pi_{\gamma\gamma}^{1\ell, W}(0)$, is in fact gauge dependent, and only when computed in the unitary gauge or in the background-field gauge (or using the pinch technique) can it be directly connected to $\mathcal{P}_h^{1\ell}$ through eq. (16).

We computed the contributions to the transverse part of the photon self-energy from two-loop diagrams that involve the BSM Higgs bosons, which we denote as $\Pi_{\gamma\gamma}^{2\ell, \text{BSM}}(0)$, by feeding to **FeynArts** [50] the model file for the TSM produced by **SARAH** [40–44]. We fixed the masses and couplings of the BSM Higgs bosons to the values that correspond to either the scenario A, see eq. (12), or the scenario B, see eq. (13). We performed our calculation in the unitary gauge, including also the contributions from diagrams that involve gauge bosons together with the BSM Higgs bosons. We set the mass of the SM-like Higgs boson to zero from the start, but we introduced a fictitious photon mass to regularize some IR-divergent integrals. Next, we Taylor-expanded the self-energy in powers of the external momentum p^2 : the zeroth-order term of the expansion vanishes as a consequence of gauge invariance, while the first-order term corresponds to $\Pi_{\gamma\gamma}^{2\ell, \text{BSM}}(0)$. We evaluated the two-loop vacuum integrals using the results of ref. [51]. Finally, we sent the fictitious photon mass to zero and then took the “gaugeless limit” of vanishing EW gauge couplings, except for an overall factor α_{em} from the couplings of the external photons. For what concerns the counterterm contributions to $\Pi_{\gamma\gamma}^{2\ell, \text{BSM}}(0)$, we assumed that the charged-Higgs mass $m_{H^\pm}^2$ entering $\Pi_{\gamma\gamma}^{1\ell}(0)$ in eq. (17) is expressed in the $\overline{\text{MS}}$ scheme (the definitions of the top and W masses are irrelevant under our approximations), and we fixed the counterterm of the charged-Higgs mass to the divergent part of the one-loop self-energy $\Pi_{H^+H^-}(m_{H^\pm}^2)$.

After the computation of the two-loop BSM contributions to the photon self-energy, the genuine two-loop part of the $h\gamma\gamma$ amplitude, denoted as $\mathcal{P}_h^{2\ell, 1\text{PI}}$ in eq. (15), can be straightforwardly obtained through the LET of refs. [38, 39], by taking the derivative of $\Pi_{\gamma\gamma}^{2\ell, \text{BSM}}(0)$ w.r.t. the doublet vev v as in eq. (16). To this purpose, the masses of the BSM Higgs bosons must be set to the tree-level expressions given in eqs. (12) and (13) for the scenarios A and B, respectively. However, the calculation of the remaining contributions in eq. (15) differs according to which of the two scenarios with vanishing doublet-triplet mixing is considered, and within each scenario there are multiple options for the sets of parameters that can be treated as input, and multiple possible choices of renormalization conditions. This will be discussed in detail in sections 3.2 and 3.3. Finally, we stress that in both scenarios we cross-checked our LET-based calculation of $\mathcal{P}_h^{2\ell}$ with a direct calculation of the $h\gamma\gamma$ amplitude at vanishing external momentum, performed along the lines of the calculation of $\Pi_{\gamma\gamma}^{2\ell, \text{BSM}}(0)$ described above.

3.2 Calculation of the $h\gamma\gamma$ amplitude in the scenario A

In this scenario, the squared masses of the SM particles entering the one-loop part of the photon self-energy, eq. (17), can be expressed as $m_t^2 = y_t^2 v^2/2$, and $m_W^2 = g^2 v^2 c_\delta^{-2}/4$, see eq. (9). Recalling that $c_\delta^{-2} = 1 + 2v_T^2/v^2$, the combination of eqs. (16) and (17) yields for the SM-like part of the one-loop $h\gamma\gamma$ amplitude

$$\mathcal{P}_h^{1\ell, \text{SM}} = \frac{4}{3} Q_t^2 N_c c_\delta^{-1} - 7 c_\delta . \quad (18)$$

We remark that, differently from the case of the aligned THDM discussed in ref. [12], it is not entirely appropriate to speak of a ‘‘SM part’’ of the amplitude, because even when $\gamma = 0$ the couplings of h to fermions and gauge bosons differ from their SM counterparts by powers of c_δ . However, as mentioned earlier in section 2, for realistic values of c_δ the numerical impact of this difference is minimal. We therefore focus our two-loop calculation on the contributions of diagrams that involve the BSM scalars, and omit the contributions of diagrams that involve only SM particles.

We now move on to the calculation of the BSM part of the one-loop $h\gamma\gamma$ amplitude, which we denote as $\mathcal{P}_h^{1\ell, \text{BSM}}$, and of the associated counterterm contributions. For consistency with the two-loop calculation of the amplitude, when applying the LET theorem of eq. (16) to the one-loop photon self-energy in eq. (17) we cannot just use the tree-level expression for the charged-Higgs mass given in eq. (12). Indeed, our choice for the counterterm contributions to $\Pi_{\gamma\gamma}^{2\ell, \text{BSM}}(0)$ implies that, in the one-loop part of the photon self-energy, we must use for charged-Higgs mass the tree-level expression – in terms of $\overline{\text{MS}}$ -renormalized Lagrangian parameters – that is valid *before* we impose the minimum conditions for the scalar potential, the condition of vanishing mass for the SM-like Higgs boson, and the condition of vanishing triplet-doublet mixing:

$$\begin{aligned} \widehat{m}_{H^\pm}^2 = & \frac{1}{2} \left[\mu^2 + m_T^2 + \frac{1}{2} (\lambda_H + \lambda_{HT}) v^2 + \frac{1}{4} (\lambda_{HT} + 2 \lambda_T) v_T^2 + \frac{1}{2} \kappa_{HT} v_T \right. \\ & \left. + \sqrt{2 \kappa_{HT}^2 v^2 + \left(\mu^2 - m_T^2 + \frac{1}{2} (\lambda_H - \lambda_{HT}) v^2 + \frac{1}{4} (\lambda_{HT} - 2 \lambda_T) v_T^2 + \frac{1}{2} \kappa_{HT} v_T \right)^2} \right] . \end{aligned} \quad (19)$$

Taking the derivative w.r.t. v of the charged-Higgs contribution to the one-loop self-energy of the photon, and then removing the parameters μ^2 , m_T^2 , λ_H and κ_{HT} by means of the tree-level conditions $\tau_H = \tau_T = m_h^2 = (\mathcal{M}_0^2)_{12} = 0$ – where τ_H and τ_T are given in eqs. (3) and (4), respectively, $m_h^2 = \lambda_H v^2$, and $(\mathcal{M}_0^2)_{12}$ is given in eq. (5) – would lead to $\mathcal{P}_h^{1\ell, \text{BSM}} = c_\delta/3$. However, in the two-loop calculation of the $h\gamma\gamma$ amplitude we need to ensure that all parameters entering the one-loop amplitude are consistently renormalized at the one-loop level. In particular, we require

$$\tau_H + T_h = 0 , \quad \tau_T + T_H = 0 , \quad m_h^2 - \frac{T_h}{v} + \Pi_{hh}(0) = 0 , \quad (\mathcal{M}_0^2)_{12} + \Pi_{hH}(0) = 0 , \quad (20)$$

where: τ_H, τ_T, m_h^2 and $(\mathcal{M}_0^2)_{12}$ are expressed in terms of $\overline{\text{MS}}$ -renormalized parameters; T_h and T_H are the finite parts of the one-loop tadpole diagrams⁷ for the neutral scalars; $\Pi_{hh}(0)$ and $\Pi_{hH}(0)$ are the finite parts of the (1, 1) and (1, 2) entries of the one-loop self-energy matrix for the neutral scalars, evaluated at vanishing external momentum. Explicit formulas for the one-loop tadpoles and self-energies, under the approximations relevant to our two-loop calculation, are listed in the appendix A. The first two conditions in eq. (20) above imply that v and v_T are the vevs of the loop-corrected effective potential, the third condition implies that the *pole* mass of the SM-like Higgs boson is vanishing, while the fourth condition implies that the doublet-triplet mixing term in the loop-corrected mass matrix for the neutral scalars vanishes for the external momentum that is relevant to the calculation of the $h \rightarrow \gamma\gamma$ decay width. At the next-to-leading order (NLO) in the loop expansion, we thus find

$$\frac{2\pi v c_\delta^{-1}}{\alpha_{\text{em}}} \frac{d\Pi_{\gamma\gamma}^{1\ell, H^\pm}(0)}{dv} = \frac{c_\delta}{3} + \Delta\mathcal{P}_h^{1\ell, \text{BSM}}, \quad (21)$$

where

$$\Delta\mathcal{P}_h^{1\ell, \text{BSM}} = -\frac{s_\delta t_\delta}{6 m_{H^\pm}^2} \left[\Pi_{hh}(0) - (3 + 2c_{2\delta}) \frac{T_h}{v} - 2t_\delta^{-3} \left(\Pi_{hH}(0) - 2c_{2\delta} \frac{T_H}{v} \right) \right]. \quad (22)$$

We can then set $\mathcal{P}_h^{1\ell, \text{BSM}} = c_\delta/3$, while $\Delta\mathcal{P}_h^{1\ell, \text{BSM}}$ becomes part of $\mathcal{P}_h^{2\ell}$ as the second contribution in eq. (15).

The third contribution to the two-loop $h\gamma\gamma$ amplitude in eq. (15) comes from the choice of renormalization scheme for the parameters entering the one-loop amplitude. In the scenario A, $\mathcal{P}_h^{1\ell}$ depends only on c_δ , which is in turn a combination of v and v_T . The various possible ways to associate the doublet and triplet vevs (together with the EW gauge couplings) to a set of physical input parameters have been extensively discussed in early studies of the EW precision observables in the TSM, see refs. [15–23]. In this work we follow the approach advocated in ref. [21], i.e., we treat the measured value of the Fermi constant G_μ and the $\overline{\text{MS}}$ -renormalized triplet vev v_T as input parameters, while we treat the doublet vev v (and, consequently, c_δ) as a derived quantity. In practice, we exploit the relation

$$c_\delta^2 = 1 - 2\sqrt{2} G_\mu v_T^2 \quad (23)$$

to obtain

$$\delta\mathcal{P}_h^{1\ell} = -\frac{t_\delta^2}{2} \left(\frac{1}{3} c_\delta - \frac{4}{3} Q_t^2 N_c c_\delta^{-1} - 7c_\delta \right) \left(\frac{\delta G_\mu}{G_\mu} + 2 \frac{\delta v_T}{v_T} \right), \quad (24)$$

where for a parameter x in a generic renormalization scheme R we define $x^R = x^{\overline{\text{MS}}} - \delta x$. Our choice of renormalization conditions corresponds then to $\delta v_T = 0$, and, under our approximations for the two-loop calculation,

$$\frac{\delta G_\mu}{G_\mu} = -\frac{\Pi_{WW}^{\text{BSM}}(0)}{m_W^2}, \quad (25)$$

⁷Decomposing the effective potential as $V_0 + \Delta V$, we also have $T_\varphi = d\Delta V/d\varphi$. Note that in the limit of vanishing doublet-triplet mixing, $\gamma = 0$, we can identify directly ϕ_H^0 with h and ϕ_T^0 with H .

where $\Pi_{WW}^{\text{BSM}}(0)$ denotes the finite part of the BSM contribution to the W self-energy at vanishing external momentum, an explicit formula for which is given in the appendix A.

The fourth contribution to the two-loop amplitude $\mathcal{P}_h^{2\ell}$ in eq. (15), i.e., $K_r \mathcal{P}_h^{1\ell}$, arises from the diagonal wave-function renormalization (WFR) of the external Higgs field and from the renormalization of the ratio $c_\delta/v \propto G_\mu^{1/2}$ that is factored out of the amplitude in eq. (16):

$$K_r = \frac{1}{2} \left(\delta Z_{hh} + \frac{\delta G_\mu}{G_\mu} \right), \quad (26)$$

where δG_μ is given in eq. (25), and

$$\delta Z_{hh} = \left. \frac{d\Pi_{hh}(p^2)}{dp^2} \right|_{p^2=0}, \quad (27)$$

$\Pi_{hh}(p^2)$ being the diagonal self-energy for the SM-like Higgs scalar at external momentum p^2 . An explicit formula for δZ_{hh} is given in the appendix A.

Combining the four contributions in eq. (15) we obtain an explicit formula for $\mathcal{P}_h^{2\ell}$ that, by making use of the tree-level expressions for the BSM Higgs masses in eq. (12), we can write in terms of λ_{HT} , δ , and the ratio $m_H^2/m_{H^\pm}^2$ (or, in alternative, λ_{HT} , λ_T , and δ). As the dependence on δ is quite involved, we relegate this result to the appendix B. We remark here that $\mathcal{P}_h^{2\ell}$ does not depend explicitly on the renormalization scale, which is consistent with the fact that the parameter c_δ entering $\mathcal{P}_h^{1\ell}$ is itself scale-independent when only the corrections controlled by λ_{HT} and λ_T are considered. We also remark that in the limit $\delta \rightarrow 0$ the BSM Higgs contribution to the two-loop $h\gamma\gamma$ amplitude reduces to

$$\mathcal{P}_h^{2\ell} \Big|_{\delta \rightarrow 0} = \frac{17 \lambda_{HT}}{144 \pi^2}. \quad (28)$$

In view of the smallness of v_T (and hence δ) in realistic EWSB scenarios, the approximation in eq. (28) can be expected to hold reasonably well even when $\delta \neq 0$. Remarkably, eq. (28) shows that, in the scenario A, $\mathcal{P}_h^{2\ell}$ can become comparable in size with the charged-Higgs contribution to $\mathcal{P}_h^{1\ell}$ when the coupling λ_{HT} approaches the upper bounds discussed at the end of section 2.

3.3 Calculation of the $h\gamma\gamma$ amplitude in the scenario B

In this scenario, characterized by the condition $\kappa_{HT} = v_T = 0$, the doublet and triplet scalars do not mix, the doublet has SM-like couplings to fermions and to gauge bosons, and the charged and neutral components of the triplet have degenerate masses at the tree level, $m_{H^\pm}^2 = m_H^2 = m_T^2 + \lambda_{HT} v^2/2$. The one-loop $h\gamma\gamma$ amplitude in the limit of vanishing m_h can again be obtained from the combination of eqs. (16) and (17), now setting $c_\delta = 1$ in the former. Differently from the case of the scenario A, the amplitude $\mathcal{P}_h^{1\ell}$ can be truly decomposed into SM and BSM parts:

$$\mathcal{P}_h^{1\ell, \text{SM}} = \frac{4}{3} Q_t^2 N_c - 7 = -\frac{47}{9}, \quad (29)$$

$$\mathcal{P}_h^{1\ell, \text{BSM}} = \frac{\lambda_{HT} v^2}{6 m_{H^\pm}^2} \quad (30)$$

$$= \frac{1}{3} \left(1 - \frac{m_T^2}{m_{H^\pm}^2} \right). \quad (31)$$

Beyond the LO, the two expressions for $\mathcal{P}_h^{1\ell, \text{BSM}}$ in eqs. (30) and (31) are equivalent to each other when all of the parameters involved are interpreted as $\overline{\text{MS}}$, but we will see below that the equivalence is broken for a different choice of renormalization scheme.

Our results for the two-loop part of the $h\gamma\gamma$ amplitude are remarkably compact in this scenario. For the BSM contribution to the two-loop self-energy of the photon we find

$$\Pi_{\gamma\gamma}^{2\ell, \text{BSM}}(0) = -\frac{\alpha_{\text{em}}}{192\pi^3} \left[\frac{\lambda_{HT}^2 v^2}{2 m_{H^\pm}^2} \left(1 - 2 \ln \frac{m_{H^\pm}^2}{Q^2} \right) + 5 \lambda_T \left(1 - \ln \frac{m_{H^\pm}^2}{Q^2} \right) \right], \quad (32)$$

where we denoted both the charged and neutral triplet masses by $m_{H^\pm}^2$. Combining directly eq. (16) and eq. (32) we obtain for the genuine two-loop part of the amplitude

$$\mathcal{P}_h^{2\ell, \text{1PI}} = \frac{\lambda_{HT} v^2}{96\pi^2 m_{H^\pm}^2} \left\{ \lambda_{HT} \left[2 - \frac{m_T^2}{m_{H^\pm}^2} \left(3 - 2 \ln \frac{m_{H^\pm}^2}{Q^2} \right) \right] + 5 \lambda_T \right\}. \quad (33)$$

We remark that in the scenario B we do not need to introduce a contribution to the two-loop $h\gamma\gamma$ amplitude analogous to the one in eq. (22). Differently from the case of the scenario A, we do not use the minimum conditions of the scalar potential to remove m_T^2 from the expression of the $\overline{\text{MS}}$ -renormalized mass $m_{H^\pm}^2$ entering the one-loop amplitude, and the condition of vanishing doublet-triplet mixing is preserved beyond the tree level by the Z_2 symmetry.

The third contribution to the two-loop $h\gamma\gamma$ amplitude in eq. (15) accounts for our choices of renormalization scheme for the parameters entering $\mathcal{P}_h^{1\ell, \text{BSM}}$ in eqs. (30) and (31). We interpret the mass of the charged Higgs boson as the pole mass $M_{H^\pm}^2$, which is related to the $\overline{\text{MS}}$ mass $m_{H^\pm}^2$ by

$$M_{H^\pm}^2 = m_{H^\pm}^2 + \Pi_{H^+H^-}(m_{H^\pm}^2), \quad (34)$$

where the self-energy of the charged Higgs boson reads

$$\Pi_{H^+H^-}(m_{H^\pm}^2) = \frac{1}{16\pi^2} \left[\lambda_{HT}^2 v^2 \left(\ln \frac{m_{H^\pm}^2}{Q^2} - 2 \right) + 5 \lambda_T m_{H^\pm}^2 \left(\ln \frac{m_{H^\pm}^2}{Q^2} - 1 \right) \right]. \quad (35)$$

Concerning the remaining parameters in eqs. (30) and (31), we interpret λ_{HT} and m_T^2 as $\overline{\text{MS}}$ -renormalized parameters⁸ at the generic renormalization scale Q . The squared vev v^2 can be directly defined as $(\sqrt{2} G_\mu)^{-1}$ without affecting the calculation of $\delta\mathcal{P}_h^{1\ell}$, because in the scenario B we find

⁸An alternative scheme in which a parameter analogous to m_T^2 is connected to the renormalized hHH vertex was considered in ref. [13] for a variant of the THDM.

$\Pi_{WW}^{\text{BSM}}(0) = 0$ under the approximations relevant to our two-loop calculation, hence $\delta G_\mu = 0$, see eq. (25). However, the result for $\delta \mathcal{P}_h^{1\ell}$ depends on whether we choose to express the BSM contribution to the one-loop amplitude as in eq. (30) or as in eq. (31):

$$\delta \mathcal{P}_h^{1\ell} \Big|_{\lambda_{HT}} = \frac{\lambda_{HT} v^2}{6 m_{H^\pm}^4} \Pi_{H^+H^-}(m_{H^\pm}^2), \quad (36)$$

$$\delta \mathcal{P}_h^{1\ell} \Big|_{m_T^2} = -\frac{m_T^2}{3 m_{H^\pm}^4} \Pi_{H^+H^-}(m_{H^\pm}^2). \quad (37)$$

In the scenario B the parameter K_r defined in eq. (26) receives only the contribution of the WFR of the external Higgs field, because $\delta G_\mu = 0$ as mentioned above. We thus find

$$K_r = -\frac{\lambda_{HT}^2 v^2}{128\pi^2 m_{H^\pm}^2}, \quad (38)$$

and the fourth contribution to the two-loop amplitude $\mathcal{P}_h^{2\ell}$ in eq. (15) becomes $K_r (\mathcal{P}_h^{1\ell, \text{SM}} + \mathcal{P}_h^{1\ell, \text{BSM}})$, where the SM and BSM contributions to the one-loop amplitude are given in eqs. (29)–(31).⁹

Combining all of the results in eqs. (29)–(38), we obtain two alternative expressions for the total BSM contribution to the $h\gamma\gamma$ amplitude, i.e., $\mathcal{P}_h^{\text{BSM}} = \mathcal{P}_h^{1\ell, \text{BSM}} + \mathcal{P}_h^{2\ell}$, depending of whether we express the one-loop part in terms of λ_{HT} or of m_T^2 :

$$\mathcal{P}_h^{\text{BSM}} \Big|_{\lambda_{HT}} = \frac{\lambda_{HT} v^2}{6 M_{H^\pm}^2} + \frac{\lambda_{HT} v^2}{96\pi^2 m_{H^\pm}^2} \left[\lambda_{HT} \left(\frac{35}{12} + 2 \ln \frac{m_{H^\pm}^2}{Q^2} \right) - \frac{5\lambda_{HT}^2 v^2}{8 m_{H^\pm}^2} + 5 \lambda_T \ln \frac{m_{H^\pm}^2}{Q^2} \right], \quad (39)$$

$$\mathcal{P}_h^{\text{BSM}} \Big|_{m_T^2} = \frac{1}{3} \left(1 - \frac{m_T^2}{M_{H^\pm}^2} \right) + \frac{1}{48\pi^2} \left[\frac{(m_{H^\pm}^2 - m_T^2)^2}{6 m_{H^\pm}^2 v^2} \left(68 + 15 \frac{m_T^2}{m_{H^\pm}^2} \right) + 5 \lambda_T \left(1 - \frac{m_T^2}{m_{H^\pm}^2} \ln \frac{m_{H^\pm}^2}{Q^2} \right) \right]. \quad (40)$$

We remark that in the two-loop parts of eqs. (39) and (40) we made use of the tree-level formula for the mass of the charged Higgs boson to express either m_T^2 or λ_{HT} in terms of the remaining parameters. Also, while the one-loop parts of eqs. (39) and (40) are explicitly expressed in terms of the pole mass $M_{H^\pm}^2$, in the two-loop parts we denote the charged-Higgs mass as $m_{H^\pm}^2$, to stress that its definition there amounts to a higher-order effect.

As we should expect from the overall scale independence of $\Gamma(h \rightarrow \gamma\gamma)$, we find that the explicit scale dependence of the two-loop part of $\mathcal{P}_h^{\text{BSM}}$ in eqs. (39) and (40) is compensated for by the implicit

⁹Since this is already a two-loop contribution, it does not matter whether we use eq. (30) or eq. (31) for $\mathcal{P}_h^{1\ell, \text{BSM}}$.

scale dependence of the parameters entering the one-loop part. The relevant terms in the RGEs of λ_{HT} and m_T^2 are [49]

$$\frac{d\lambda_{HT}}{d\ln Q^2} \supset \frac{\lambda_{HT}}{16\pi^2} (2\lambda_{HT} + 5\lambda_T), \quad \frac{dm_T^2}{d\ln Q^2} \supset \frac{5\lambda_T}{16\pi^2} m_T^2, \quad (41)$$

while the one-loop RGE for v does not depend on the quartic Higgs couplings, and the pole mass $M_{H^\pm}^2$ is obviously scale-independent.

Finally, it might be worth discussing the behavior of $\mathcal{P}_h^{\text{BSM}}$ in the two limiting cases $m_T^2 \rightarrow 0$, where $m_{H^\pm}^2 \rightarrow \lambda_{HT} v^2/2$, and $m_T^2 \rightarrow \infty$, where also $m_{H^\pm}^2 \rightarrow \infty$. For vanishing m_T^2 , the expression for $\mathcal{P}_h^{\text{BSM}}$ that depends explicitly on that parameter, eq. (40), becomes

$$\mathcal{P}_h^{\text{BSM}} \Big|_{m_T^2 \rightarrow 0} = \frac{1}{3} + \frac{17\lambda_{HT} + 15\lambda_T}{144\pi^2}. \quad (42)$$

We note a discrepancy with the two-loop contribution to the $h\gamma\gamma$ amplitude obtained in the scenario A for the limit $\delta \rightarrow 0$, see eq. (28), in seeming contradiction with the tree-level expectation that this limit should correspond to $m_T^2 \rightarrow 0$. This is due to the fact that, at the perturbative order required for consistency with the two-loop calculation of the amplitude, the limit $\delta \rightarrow 0$ in the scenario A corresponds in fact to $m_T^2 \rightarrow 5\lambda_{HT}\lambda_T v^2/(32\pi^2)$, as can be checked by combining eqs. (4), (20), (A2) and (A4). If we take the latter limit in eq. (40), we do indeed reproduce eq. (28). We also note that in the expression for $\mathcal{P}_h^{\text{BSM}}$ that depends on λ_{HT} , eq. (39), the two-loop part does not coincide with eq. (42) when we set $m_{H^\pm}^2 = \lambda_{HT} v^2/2$. This is however compensated for by the fact that the one-loop part does not in turn tend to $1/3$ for $m_T^2 \rightarrow 0$, because in that limit the pole mass $M_{H^\pm}^2$ differs from $\lambda_{HT} v^2/2$ by a one-loop shift, see eqs. (34) and (35). In other words, the expected limit is reproduced also in eq. (39), but only by the sum of the one- and two-loop parts.

In the opposite limit, $m_T^2 \rightarrow \infty$, the expression for $\mathcal{P}_h^{\text{BSM}}$ that depends on λ_{HT} tends manifestly to zero, reflecting the expected decoupling of the heavy triplet states from the properties of the SM-like Higgs boson, because all terms in eq. (39) are suppressed by powers of $v^2/m_{H^\pm}^2$. In contrast, the decoupling is not manifest in the expression for $\mathcal{P}_h^{\text{BSM}}$ that depends on m_T^2 , eq. (40), where the term proportional to λ_T in the two-loop part does not vanish. However, this is compensated for by the one-loop part, which does not vanish either when $m_T^2 \rightarrow \infty$ due to a non-decoupling term in the relation between $M_{H^\pm}^2$ and $m_{H^\pm}^2$, see eqs. (34) and (35). Once again, eq. (40) does reproduce the expected decoupling of the heavy triplet states, but only in the sum of the one- and two-loop parts.

An alternative way to make the decoupling of heavy states manifest in the two-loop corrections even when using an expression for $\mathcal{P}_h^{\text{BSM}}$ similar to eq. (40) was discussed in refs. [10, 11], in the context of the two-loop calculation of the Higgs self-couplings in the THDM. In those studies it was proposed that the non-decoupling terms be absorbed in a redefinition of the parameter that controls the mass of the heavy states. Following that approach, we can define $(m_T^2)^{\text{dec}} = (m_T^2)^{\overline{\text{MS}}} + \delta m_T^2$, where

$$\delta m_T^2 = -\frac{5\lambda_T}{16\pi^2} m_T^2 \left(1 - \ln \frac{m_T^2}{Q^2} \right), \quad (43)$$

and we obtain for the BSM contribution to the $h\gamma\gamma$ amplitude

$$\mathcal{P}_h^{\text{BSM}} \Big|_{(m_T^2)^{\text{dec}}} = \frac{1}{3} \left(1 - \frac{(m_T^2)^{\text{dec}}}{M_{H^\pm}^2} \right) + \frac{1}{48\pi^2} \left\{ \frac{(m_{H^\pm}^2 - m_T^2)^2}{6 m_{H^\pm}^2 v^2} \left(68 + 15 \frac{m_T^2}{m_{H^\pm}^2} \right) + 5 \lambda_T \left[1 - \frac{m_T^2}{m_{H^\pm}^2} \left(1 + \ln \frac{m_{H^\pm}^2}{m_T^2} \right) \right] \right\}. \quad (44)$$

The two-loop part of $\mathcal{P}_h^{\text{BSM}}$ in eq. (44) now vanishes when $m_T^2 \rightarrow \infty$, because in that limit $m_{H^\pm}^2 \approx m_T^2$ (again, we denote the mass parameters in the two-loop part as $m_{H^\pm}^2$ and m_T^2 because their definitions there amount to higher-order effects). On the other hand, the vanishing of the one-loop part for $(m_T^2)^{\text{dec}} \rightarrow \infty$ results from the combination of eqs. (34), (35) and (43).

4 Numerical impact of the two-loop BSM contributions to $\Gamma[h \rightarrow \gamma\gamma]$

We now illustrate the numerical impact of the newly-computed two-loop corrections on the prediction for $\Gamma[h \rightarrow \gamma\gamma]$ in the TSM. We focus on the two scenarios described in the previous sections, in which the neutral components of doublet and triplet do not mix, so that the lighter neutral scalar h has SM-like couplings to fermions and gauge bosons and plays the role of the 125-GeV Higgs boson discovered at the LHC. A comprehensive analysis of the parameter space of the model along the lines of refs. [24–32], taking into account all of the theoretical and experimental constraints, is well beyond the scope of this paper. What we aim to discuss here, at the qualitative level, is how the inclusion of the two-loop corrections controlled by the couplings λ_{HT} and λ_T can affect the prediction for $\Gamma[h \rightarrow \gamma\gamma]$ in scenarios where those couplings are large. To this purpose, we can neglect all of the two-loop corrections controlled by the SM couplings, which are of $\mathcal{O}(1)$ or smaller. The inclusion of those corrections as computed for the SM¹⁰ would refine our prediction for $\Gamma[h \rightarrow \gamma\gamma]$, but would not alter our qualitative conclusions on the relevance of the two-loop corrections in scenarios with large scalar couplings.

The LHC average of the signal strength for the production of the 125-GeV Higgs boson followed by its decay to a pair of photons is [3]

$$\mu_{\gamma\gamma}^{\text{exp}} \equiv \frac{\sigma^{\text{exp}}(pp \rightarrow h) \text{BR}^{\text{exp}}(h \rightarrow \gamma\gamma)}{\sigma^{\text{SM}}(pp \rightarrow h) \text{BR}^{\text{SM}}(h \rightarrow \gamma\gamma)} = 1.10 \pm 0.07, \quad (45)$$

where the numerator of $\mu_{\gamma\gamma}^{\text{exp}}$ contains the experimental measurement, the denominator contains the SM prediction, and the branching ratio (BR) for the decay $h \rightarrow \gamma\gamma$ is defined as the ratio of the partial width $\Gamma[h \rightarrow \gamma\gamma]$ over the total width Γ_h^{tot} . Eq. (45) shows a mild (1.4σ) excess in $\mu_{\gamma\gamma}^{\text{exp}}$, driven by the CMS measurement [67]. If taken seriously, this excess would suggest some tension with any

¹⁰See refs. [52–58] for the QCD part, refs. [59–62] for the EW corrections involving the top quark, and refs. [63–66] for the remaining EW corrections.

model that predicts a positive BSM contribution to the $h\gamma\gamma$ amplitude, and thus a value of $\Gamma[h \rightarrow \gamma\gamma]$ lower than the SM prediction (note that our conventions are such that the $h\gamma\gamma$ amplitude is negative in the SM). In the case of the TSM, the one-loop contribution from the charged Higgs boson has the same sign as λ_{HT} . In the scenario A, λ_{HT} must always be positive to avoid a tachyonic mass for the charged Higgs boson, see eq. (12), whereas in the scenario B it can take either sign, but negative values are constrained by the requirement that the scalar potential be bounded from below, $\lambda_{HT} > -\sqrt{2\lambda_H\lambda_T}$. Even if the accumulation of additional data from the current and future runs of the LHC should bring the central value of the signal strength closer to the SM prediction, $\mu_{\gamma\gamma}^{\text{exp}} \approx 1$, the comparison with the prediction of the TSM will still provide significant constraints on the parameter space of the model, also in view of the expected reduction of the uncertainties [68].

To highlight the effect of the newly-computed two-loop corrections controlled by λ_{HT} and λ_T , we define simplified predictions at one and two loops for the signal-strength parameter in the TSM

$$\mu_{\gamma\gamma}^{1\ell} \equiv \frac{|\mathcal{F}_h^{1\ell}|^2}{|\mathcal{F}_h^{1\ell, \text{SM}}|^2}, \quad \mu_{\gamma\gamma}^{2\ell} \equiv \frac{\left| \mathcal{F}_h^{1\ell} \left(1 + \frac{\mathcal{P}_h^{2\ell}}{\mathcal{P}_h^{1\ell}} \right) \right|^2}{|\mathcal{F}_h^{1\ell, \text{SM}}|^2}, \quad (46)$$

where $\mathcal{F}_h^{1\ell}$ and $\mathcal{F}_h^{1\ell, \text{SM}}$ denote the one-loop, m_h -dependent $h\gamma\gamma$ amplitudes in the TSM and in the SM, respectively, and are given in the appendix C, whereas $\mathcal{P}_h^{1\ell}$ and $\mathcal{P}_h^{2\ell}$ are the one- and two-loop amplitudes for vanishing m_h in the TSM, as computed in the previous section. The way we organized the contributions in eq. (46) allows us to retain the Higgs-mass dependence of the signal-strength parameter at the LO,¹¹ while keeping into account that the two-loop corrections are known only in the limit of vanishing m_h , and should be compared with a one-loop result computed in the same limit to avoid introducing a bias. Note that an implicit assumption in eq. (46) is that the large quartic Higgs couplings do not significantly affect the ratio of production cross section over total decay width of the SM-like Higgs boson, i.e., $[\sigma(pp \rightarrow h) / \Gamma_h^{\text{tot}}]^{\text{TSM}} \approx [\sigma(pp \rightarrow h) / \Gamma_h^{\text{tot}}]^{\text{SM}}$. Indeed, the dominant NLO contributions involving those couplings affect the main production and decay channels only through the common multiplicative factor K_r , see eq. (26), which cancels in the ratio.

In figure 1 we plot the predictions for $\mu_{\gamma\gamma}$ as a function of the charged-Higgs mass in the scenario A of the TSM. We denote the mass as m_{H^\pm} , because in this scenario its definition beyond the tree level has only a higher-order effect on our two-loop calculation of $\mathcal{P}_h^{\text{BSM}}$. We set $v_T = 6.5$ GeV, close to the value that leads to a prediction for m_W in accordance with the CDF measurement [33]. Even for this value of v_T , which could be considered as an upper bound of the acceptable range, eq. (23) implies $c_\delta \approx 0.999$, and indeed we find that our prediction for $\mu_{\gamma\gamma}^{2\ell}$, see eq. (46), would vary by less than 0.1% if we used $\mathcal{P}_h^{2\ell}|_{\delta \rightarrow 0}$ from eq. (28) instead of the δ -dependent result for $\mathcal{P}_h^{2\ell}$ given in the appendix B. We can thus refer directly to eq. (28) when discussing the dependence of the two-loop corrections on the quartic Higgs couplings. This implies that, in the scenario A, the values of both v_T and λ_T have a negligible impact on the prediction for the $h\gamma\gamma$ amplitude.

¹¹This improves the definition of the simplified signal-strength parameter introduced in our ref. [12] for the THDM.

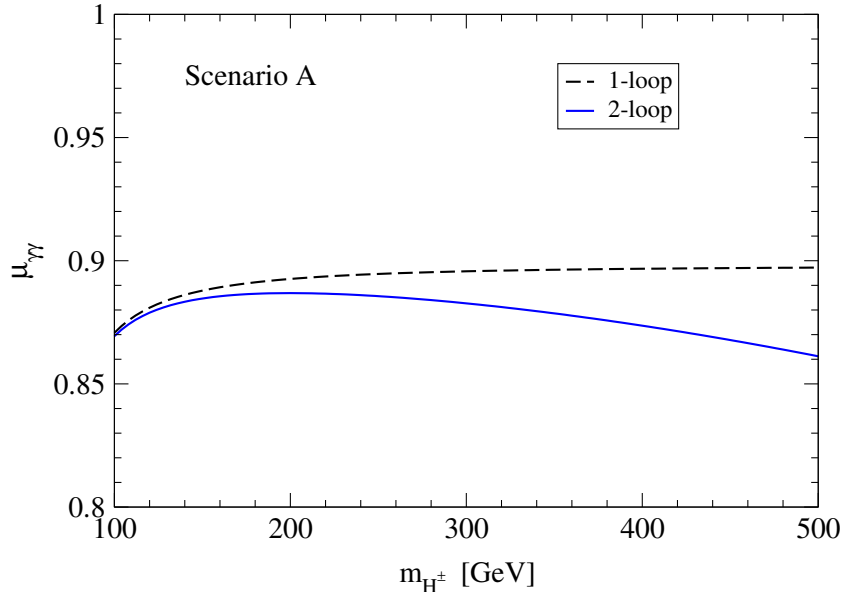


Figure 1: *Signal strength $\mu_{\gamma\gamma}$ as a function of the charged-Higgs mass in the scenario A of the TSM, with $v_T = 6.5$ GeV. The meaning of the different lines is explained in the text.*

The black dashed line in figure 1 represents the prediction for $\mu_{\gamma\gamma}^{1\ell}$, whereas the blue solid line represents the prediction for $\mu_{\gamma\gamma}^{2\ell}$. Since in the scenario A the couplings λ_{HT} and λ_T enter explicitly only the two-loop amplitude $\mathcal{P}_h^{2\ell}$, we can extract λ_{HT} from the tree-level relation $m_{H^\pm}^2 = \lambda_{HT} v^2 / (2c_\delta^2)$, and we simply fix $\lambda_T = 5$ (as mentioned above, the latter choice has a negligible impact on our results). The figure shows that the one-loop prediction for the signal strength reaches a plateau as soon as m_{H^\pm} is large enough that the BSM contribution to the $h\gamma\gamma$ amplitude is well approximated by the result in the limit of vanishing m_h , i.e., $\mathcal{P}_h^{1\ell, \text{BSM}} = c_\delta/3$. The effect of the two-loop BSM contributions manifests itself as a negative correction to the signal strength that increases in size with growing m_{H^\pm} . In view of the relation between m_{H^\pm} and λ_{HT} in the scenario A, this behavior can be directly traced back to the dependence of the two-loop corrections on λ_{HT} in the r.h.s. of eq. (28). We note that the largest value of m_{H^\pm} considered in figure 1 corresponds to $\lambda_{HT} \approx 8$, well within the upper bound from perturbative unitarity.

Comparing directly the TSM predictions in figure 1 with the measured value for the signal strength in eq. (45) would lead to the rather drastic conclusion that the scenario A is ruled out at the 3σ level for all values of m_{H^\pm} when the two-loop contributions are included (in contrast, the one-loop prediction differs from the measured value by slightly less than 3σ as soon as $m_{H^\pm} \gtrsim 170$ GeV). If we assume instead that the excess in $\mu_{\gamma\gamma}^{\text{exp}}$ is due to a statistical fluctuation, and that more data will not only shrink the experimental uncertainty band but also bring the central value of the signal strength close to one, a future 2σ exclusion line could fall right into the region spanned by the two lines in figure 1. The two-loop corrections might thus turn a scenario that was marginally allowed into an excluded one. In any case, it is clear that for large values of λ_{HT} the inclusion of the two-loop corrections is necessary to obtain an accurate prediction for the $h \rightarrow \gamma\gamma$ signal strength.

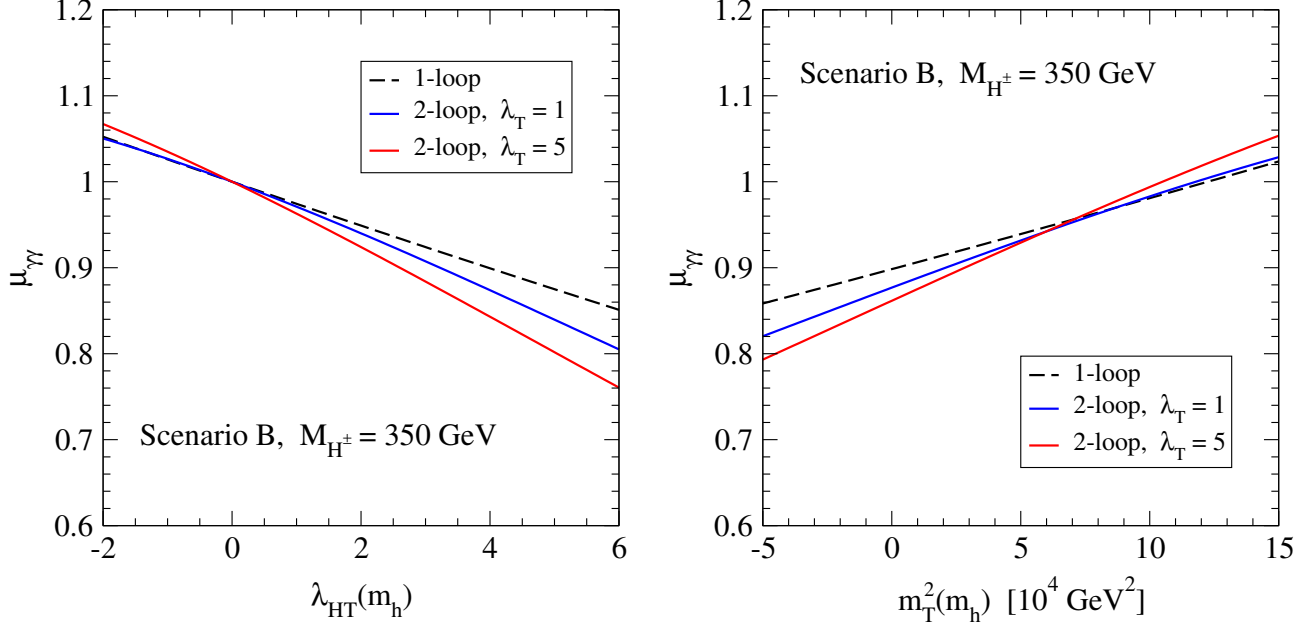


Figure 2: Signal strength $\mu_{\gamma\gamma}$ as a function of $\lambda_{HT}(m_h)$ (left) or $m_T^2(m_h)$ (right) in the scenario B of the TSM, with $M_{H^\pm} = 350$ GeV. The meaning of the different lines is explained in the text.

Moving on to the scenario B, in figure 2 we plot the predictions for $\mu_{\gamma\gamma}$ as a function of either λ_{HT} (left plot) or m_T^2 (right plot), both interpreted as $\overline{\text{MS}}$ -renormalized parameters at the scale $Q = m_h$. We fix the pole mass of the charged Higgs boson, which enters the one-loop part of the $h\gamma\gamma$ amplitude in eqs. (39) and (40), to $M_{H^\pm} = 350$ GeV, a value that according to refs. [27, 28] should be within reach of the current searches for disappearing tracks at the LHC. In each plot, the black dashed line represents the prediction for $\mu_{\gamma\gamma}^{1\ell}$, whereas the blue and red solid lines represent the predictions for $\mu_{\gamma\gamma}^{2\ell}$ when $\lambda_T = 1$ and $\lambda_T = 5$, respectively. The requirements that the scalar potential be bounded from below and that the SM-like minimum be global imply $-0.7 \lesssim \lambda_{HT} \lesssim 4.8$ and $-2 \times 10^4 \text{ GeV}^2 \lesssim m_T^2 \lesssim 14 \times 10^4 \text{ GeV}^2$ when $\lambda_T = 1$, and $-1.6 \lesssim \lambda_{HT} \lesssim 5.7$ and $-5 \times 10^4 \text{ GeV}^2 \lesssim m_T^2 \lesssim 17 \times 10^4 \text{ GeV}^2$ when $\lambda_T = 5$. However, we stress that these bounds are derived from tree-level relations and should be treated as merely qualitative, and that the upper (lower) bounds on λ_{HT} (on m_T^2) could be somewhat relaxed by allowing for a metastable SM-like vacuum.

In the left plot in figure 2, the comparison between the three lines shows that the two-loop corrections can be quite relevant in this scenario, and that their size increases for increasing λ_T . For example, if we assumed that the “true” central value of the signal strength is exactly one, the current 2σ exclusion line would sit at $\mu_{\gamma\gamma} = 0.86$. The comparison with the TSM prediction would thus rule out $\lambda_{HT} \gtrsim 5.6$ when based on the one-loop calculation of the $h\gamma\gamma$ amplitude, $\lambda_{HT} \gtrsim 4.4$ when based on the two-loop calculation with $\lambda_T = 1$, and $\lambda_{HT} \gtrsim 3.6$ when based on the two-loop calculation with $\lambda_T = 5$. The impact of the two-loop corrections in the right plot in figure 2 is qualitatively similar to the one shown in the left plot: a 2σ exclusion line at $\mu_{\gamma\gamma} = 0.86$ would rule out $m_T^2 \lesssim -5 \times 10^4 \text{ GeV}^2$ when based on the one-loop calculation, $m_T^2 \lesssim -1.5 \times 10^4 \text{ GeV}^2$ when based on the two-loop calculation with $\lambda_T = 1$, and $m_T^2 \lesssim 0$ when based on the two-loop calculation with $\lambda_T = 5$.

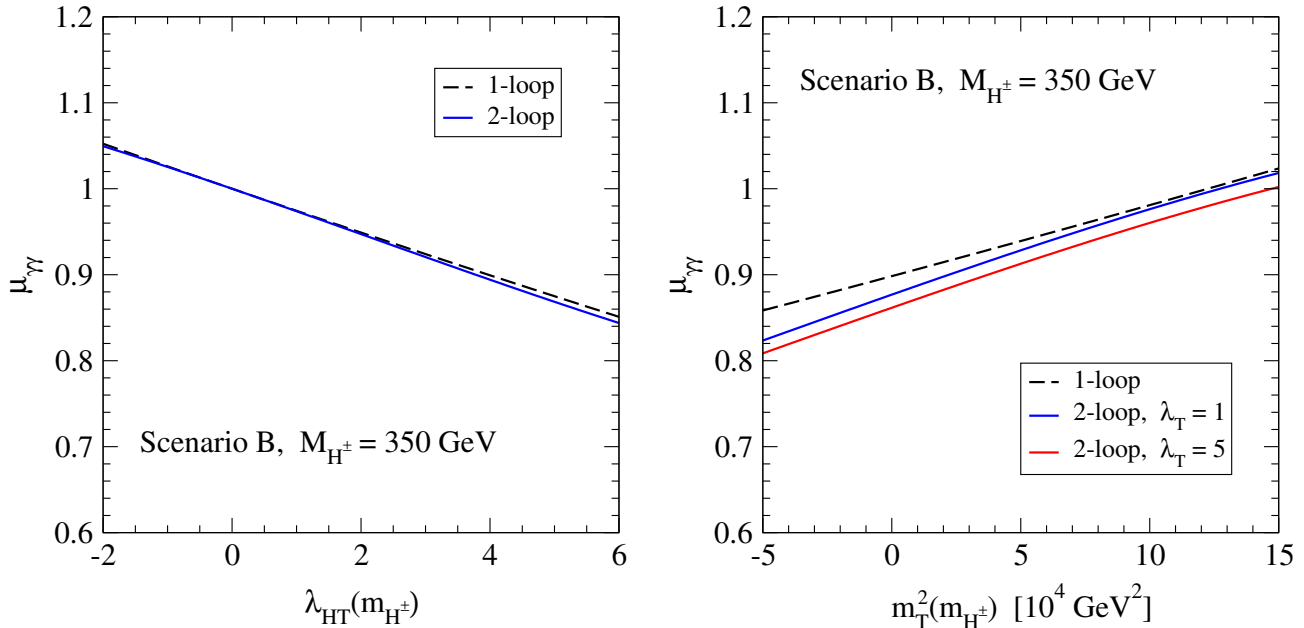


Figure 3: Same as figure 2, but the parameters on the x-axis are computed at $Q = m_{H^\pm}$.

Finally, in figure 3 we plot the same quantities as in figure 2, but as function of $\overline{\text{MS}}$ -renormalized parameters at the scale $Q = m_{H^\pm}$ instead of $Q = m_h$ (note that changing the input scale amounts to considering a different region of the TSM parameter space). We see that in the left plot of figure 3 – where the signal strength is shown as a function of $\lambda_{HT}(m_{H^\pm})$ – the two-loop corrections are now significantly smaller, and they do not depend at all on λ_T . Inspection of eq. (39) shows indeed that the λ_T -dependent part of $\mathcal{P}_h^{2\ell}$ is entirely proportional to $\ln(m_{H^\pm}^2/Q^2)$, and that there happens to be a significant cancellation between the non-logarithmic terms in the λ_T -independent part. Therefore, taking $\lambda_{HT}(m_{H^\pm})$ as input parameter in phenomenological analyses of this scenario might look like the most convenient choice, because it reduces the dimensionality of the parameter space on which the two-loop prediction for $\mu_{\gamma\gamma}$ depends. In contrast, we see that in the right plot – where the signal strength is shown as a function of $m_T^2(m_{H^\pm})$ – the two-loop corrections remain significant. Inspection of eq. (40) shows indeed that in this case the choice $Q = m_{H^\pm}$ does not entirely kill off the λ_T -dependent part of $\mathcal{P}_h^{2\ell}$, and that the λ_T -independent part does not depend at all on the scale. This said, we stress that the choice of input parameters always depends on the kind of analysis that is being performed, and that there might be compelling reasons to pick a parameter other than $\lambda_{HT}(m_{H^\pm})$.

5 Conclusions

The requirement that an extension of the SM accommodate a scalar with properties compatible with those observed at the LHC constrains the parameter space of the BSM model even before the direct observation of any new particles. In models with an extended Higgs sector, some of the quartic scalar couplings can be significantly larger than any of the SM couplings, while still satisfying all of the

theoretical and experimental constraints. In such cases, the radiative corrections controlled by those couplings can be expected to be the dominant ones, and their inclusion may prove necessary in order to obtain accurate predictions for the properties of the observed Higgs boson.

In this paper we computed the two-loop BSM contributions to $\Gamma(h \rightarrow \gamma\gamma)$ in the TSM, a model in which the Higgs sector of the SM is augmented with a real triplet of $SU(2)$. We considered two scenarios in which the neutral components of doublet and triplet do not mix, so that the lighter neutral scalar h has (at least approximately) SM-like couplings to fermions and gauge bosons. Following the approach of our ref. [12], where an analogous calculation was performed for the THDM, we focused on the corrections controlled by the potentially large scalar couplings, and we made use of a LET that connects the $h\gamma\gamma$ amplitude to the derivative of the photon self-energy w.r.t. the vev of the SM-like Higgs field. This allowed us to obtain explicit and compact formulas for the two-loop BSM contributions to the $h\gamma\gamma$ amplitude in the two considered scenarios.

After describing our calculation, we briefly illustrated the numerical impact of the newly-computed two-loop BSM contributions. We chose not to embark in an extensive analysis of the TSM parameter space, but rather discuss, at the qualitative level, how the inclusion of the two-loop corrections controlled by the quartic scalar couplings can be necessary in order to obtain a precise prediction for $\Gamma[h \rightarrow \gamma\gamma]$ in scenarios where those couplings are large. We defined a simplified signal-strength parameter $\mu_{\gamma\gamma}$, and showed how the inclusion of the two-loop BSM contributions tends to exacerbate the tension between the measured value of the signal strength, which is in fact slightly above the SM prediction, and the prediction of the TSM in the considered scenarios, which is somewhat below the SM prediction. We also discussed how, in one of the considered scenarios, the relevance of the two-loop corrections depends on which parameters are used as input for the one-loop part of the $h\gamma\gamma$ amplitude, and we identified a choice that might prove more convenient than the others.

What we presented here is, to the best of our knowledge, the first calculation of two-loop corrections to the properties of the Higgs boson in the TSM, and our investigation could obviously be extended in multiple directions. To start with, our results for $\Gamma[h \rightarrow \gamma\gamma]$ could be generalized to the case of a non-zero (but necessarily small) mixing between the neutral components of doublet and triplet, which would entail a number of complications related to the renormalization of the mixing angle. Beyond $\Gamma[h \rightarrow \gamma\gamma]$, the techniques we developed could also be used to compute the two-loop BSM contributions to the ρ parameter, in analogy with the THDM calculation of refs. [7, 8], and to the trilinear self-coupling λ_{hhh} , in analogy with the THDM calculation of refs. [10, 11]. We hope that the results presented in this paper will help the collective effort to use the properties of the Higgs boson as a probe of what lies beyond the SM.

Acknowledgments

We thank M. Goodsell for useful communications about the implementation of the TSM in SARAH.

Appendix A: One-loop tadpoles and self-energies in the scenario A

In this appendix we list explicit formulas for the finite parts of the one-loop tadpoles and self-energies that are relevant to our calculation. They were obtained by adapting to the TSM the general formulas given in refs. [69, 70], under the limits of vanishing doublet-triplet mixing angle γ , vanishing SM-like Higgs mass, and vanishing gauge and Yukawa couplings (except for an overall factor g^2 in the BSM contribution to the W self-energy).

$$16\pi^2 T_h = -\frac{\lambda_{HT} v}{2} \left[2 m_{H^\pm}^2 \left(1 - \ln \frac{m_{H^\pm}^2}{Q^2} \right) + m_H^2 \left(1 - \ln \frac{m_H^2}{Q^2} \right) \right], \quad (\text{A1})$$

$$16\pi^2 T_H = (\lambda_{HT} s_\delta^2 + \lambda_T c_\delta^2) v t_\delta m_{H^\pm}^2 \left(1 - \ln \frac{m_{H^\pm}^2}{Q^2} \right) + \frac{3}{2} \lambda_T v t_\delta m_H^2 \left(1 - \ln \frac{m_H^2}{Q^2} \right), \quad (\text{A2})$$

$$16\pi^2 \Pi_{hh}(0) = -\frac{\lambda_{HT}}{2} \left[2 c_\delta^2 m_{H^\pm}^2 \left(1 - \ln \frac{m_{H^\pm}^2}{Q^2} \right) + m_H^2 \left(1 - \ln \frac{m_H^2}{Q^2} \right) \right] + \frac{\lambda_{HT}^2 v^2}{2} \left[2 \ln \frac{m_{H^\pm}^2}{Q^2} + \ln \frac{m_H^2}{Q^2} - t_\delta^2 \left(1 - \ln \frac{m_{H^\pm}^2}{Q^2} \right) \right], \quad (\text{A3})$$

$$16\pi^2 \Pi_{hH}(0) = -\frac{\lambda_{HT} v^2 t_\delta}{2} \left[2(\lambda_{HT} - \lambda_T) s_\delta^2 + \lambda_T \left(2 \ln \frac{m_{H^\pm}^2}{Q^2} + 3 \ln \frac{m_H^2}{Q^2} \right) \right], \quad (\text{A4})$$

$$16\pi^2 \left. \frac{d\Pi_{hh}(p^2)}{dp^2} \right|_{p^2=0} = -\frac{\lambda_{HT}^2 v^2}{12} \left[\frac{2 + 3 t_\delta^2}{m_{H^\pm}^2} + \frac{1}{m_H^2} \right], \quad (\text{A5})$$

$$16\pi^2 \Pi_{WW}^{\text{BSM}}(0) = -\frac{g^2}{8} \left[(3 + c_{2\delta}) m_{H^\pm}^2 + 4 m_H^2 + 8 c_\delta^2 \frac{m_{H^\pm}^2 m_H^2}{m_{H^\pm}^2 - m_H^2} \ln \frac{m_H^2}{m_{H^\pm}^2} \right]. \quad (\text{A6})$$

Note that our convention for the sign of the scalar self-energies implies $M_\phi^2 = (m_\phi^2)^{\overline{\text{MS}}} + \Pi_{\phi\phi}(m_\phi^2)$, whereas our convention for the sign of the W self-energy implies $M_W^2 = (m_W^2)^{\overline{\text{MS}}} - \Pi_{WW}(m_W^2)$.

Appendix B: Two-loop $h\gamma\gamma$ amplitude in the scenario A

We provide here an explicit formula for the two-loop $h\gamma\gamma$ amplitude $\mathcal{P}_h^{2\ell}$, valid under the assumptions of vanishing mixing between the neutral components of doublet and triplet, vanishing mass of the SM-like Higgs, and vanishing gauge and Yukawa couplings. We made use of the tree-level expressions for the BSM Higgs masses in eq. (12) to write $\mathcal{P}_h^{2\ell}$ in terms of λ_{HT} , δ , and the ratio $x \equiv m_H^2/m_{H^\pm}^2$. We remark that the latter can also be expressed as $x = c_\delta^2 + s_\delta^2 \lambda_T/\lambda_{HT}$, in which case λ_T is treated as an input parameter instead of x .

$$\begin{aligned}
\mathcal{P}_h^{2\ell} = & \frac{\lambda_{HT} c_\delta s_\delta^{-2}}{864 \pi^2 x (x-4)^2} \left\{ 520 - 8736 x + 1611 x^2 + 800 x^3 - 162 x^4 + 9 (2x^2 + 3)(x-4)^2 c_{2\delta} \right. \\
& - 2 (560 + 1752 x - 612 x^2 - 71 x^3 + 18 x^4) c_\delta^2 \\
& + 6 (64 + 1800 x - 921 x^2 + 128 x^3) c_\delta^4 \\
& + 3 x (1 + 2x) (x-4)^2 (19 + 11 c_{2\delta}) c_\delta^{-4} \\
& - \frac{12 \ln x}{(x-1)(x-4)} \left[36 + 192 x + 1703 x^2 - 1401 x^3 + 363 x^4 - 29 x^5 \right. \\
& \quad - 6 (24 - 548 x + 548 x^2 - 228 x^3 + 47 x^4 - 5 x^5) c_\delta^2 \\
& \quad + 12 (12 - 308 x + 210 x^2 - 57 x^3 + 8 x^4) c_\delta^4 \\
& \quad \left. + 8 x^2 (x-4)^3 c_\delta^{-2} \right] \\
& + \frac{216 \phi(x/4)}{x(x-4)} \left[2 + 7x - 8x^2 + 2x^3 \right. \\
& \quad - 2 (4 + 8x - 14x^2 + 6x^3 - x^4) c_\delta^2 \\
& \quad \left. + (8 + 4x - 14x^2 + 5x^3) c_\delta^4 \right] \left. \right\}. \tag{B1}
\end{aligned}$$

The function $\phi(z)$ entering eq. (B1) above is defined as

$$\phi(z) = \begin{cases} 4 \sqrt{\frac{z}{1-z}} \text{Cl}_2(2 \arcsin \sqrt{z}) \quad , & (0 < z < 1) \quad , \\ \frac{1}{\lambda} \left[-4 \text{Li}_2\left(\frac{1-\lambda}{2}\right) + 2 \ln^2\left(\frac{1-\lambda}{2}\right) - \ln^2(4z) + \pi^2/3 \right] \quad , & (z \geq 1) \quad , \end{cases} \tag{B2}$$

where $\text{Cl}_2(z) = \text{Im Li}_2(e^{iz})$ is the Clausen function, and $\lambda = \sqrt{1 - (1/z)}$.

Appendix C: Higgs-mass dependence of the one-loop $h\gamma\gamma$ amplitude

We provide here explicit formulas for the one-loop, Higgs-mass dependent $h\gamma\gamma$ amplitudes entering eq. (46), for the TSM scenarios A and B as well as for the SM. They read

$$\mathcal{F}_h^{1\ell}\Big|_A = c_\delta F_0\left(\frac{4m_{H^\pm}^2}{m_h^2}\right) + Q_t^2 N_c c_\delta^{-1} F_{1/2}\left(\frac{4m_t^2}{m_h^2}\right) + c_\delta F_1\left(\frac{4m_W^2}{m_h^2}\right), \quad (\text{A1})$$

$$\mathcal{F}_h^{1\ell}\Big|_{\lambda_{HT}} = \frac{\lambda_{HT} v^2}{2M_{H^\pm}^2} F_0\left(\frac{4m_{H^\pm}^2}{m_h^2}\right) + Q_t^2 N_c F_{1/2}\left(\frac{4m_t^2}{m_h^2}\right) + F_1\left(\frac{4m_W^2}{m_h^2}\right), \quad (\text{A2})$$

$$\mathcal{F}_h^{1\ell}\Big|_{m_T^2} = \left(1 - \frac{m_T^2}{M_{H^\pm}^2}\right) F_0\left(\frac{4m_{H^\pm}^2}{m_h^2}\right) + Q_t^2 N_c F_{1/2}\left(\frac{4m_t^2}{m_h^2}\right) + F_1\left(\frac{4m_W^2}{m_h^2}\right), \quad (\text{A3})$$

$$\mathcal{F}_h^{1\ell,\text{SM}} = Q_t^2 N_c F_{1/2}\left(\frac{4m_t^2}{m_h^2}\right) + F_1\left(\frac{4m_W^2}{m_h^2}\right), \quad (\text{A4})$$

where for the scenario B we distinguish the two cases in which the one-loop part is expressed in terms of either λ_{HT} or m_T^2 . The loop functions F_0 , $F_{1/2}$ and F_1 are

$$F_0(x) = -x \left[1 - x \left(\arcsin \frac{1}{\sqrt{x}} \right)^2 \right], \quad (\text{A5})$$

$$F_{1/2}(x) = 2x \left[1 + (1-x) \left(\arcsin \frac{1}{\sqrt{x}} \right)^2 \right], \quad (\text{A6})$$

$$F_1(x) = -2 - 3x \left[1 + (2-x) \left(\arcsin \frac{1}{\sqrt{x}} \right)^2 \right]. \quad (\text{A7})$$

In eqs. (A5)–(A7) we provide only the representations of the loop functions valid when $x \geq 1$, because we neglect the tiny contributions of the light fermions and we consider only scenarios where $m_{H^\pm} > m_h/2$. The limits of the loop functions for $x \rightarrow \infty$ are $F_0(x) \rightarrow 1/3$, $F_{1/2}(x) \rightarrow 4/3$, and $F_1(x) \rightarrow -7$, so that for vanishing m_h we recover eqs. (18) and (21) for the scenario A and eqs. (29)–(31) for the scenario B. Our notation for the mass of the charged Higgs boson is meant to stress that its one-loop definition is relevant only for the pre-factor of F_0 in eqs. (A2) and (A3), where it must be interpreted as the pole mass. For the SM-particle masses entering eqs. (A1)–(A4) and for the Fermi constant¹² we use the current PDG values [3], i.e., $m_h = 125.25$ GeV, $m_t = 172.69$ GeV, $m_W = 80.377$ GeV, and $G_\mu = 1.16638 \times 10^{-5}$ GeV⁻².

¹²The value of G_μ is needed to obtain c_δ in the scenario A and v in the scenario B.

References

- [1] **CMS** Collaboration, S. Chatrchyan *et al.*, *Observation of a New Boson at a Mass of 125 GeV with the CMS Experiment at the LHC*. Phys. Lett. B **716** (2012) 30–61, [arXiv:1207.7235](#) [hep-ex].
- [2] **ATLAS** Collaboration, G. Aad *et al.*, *Observation of a new particle in the search for the Standard Model Higgs boson with the ATLAS detector at the LHC*. Phys. Lett. B **716** (2012) 1–29, [arXiv:1207.7214](#) [hep-ex].
- [3] **Particle Data Group** Collaboration, R. L. Workman *et al.*, *Review of Particle Physics*. PTEP **2022** (2022) 083C01.
- [4] J. F. Gunion, H. E. Haber, G. L. Kane, and S. Dawson, *The Higgs Hunter's Guide*. Front. Phys. **80** (2000) .
- [5] M. Aoki, S. Kanemura, K. Tsumura, and K. Yagyu, *Models of Yukawa interaction in the two Higgs doublet model, and their collider phenomenology*. Phys. Rev. D **80** (2009) 015017, [arXiv:0902.4665](#) [hep-ph].
- [6] G. C. Branco, P. M. Ferreira, L. Lavoura, M. N. Rebelo, M. Sher, and J. P. Silva, *Theory and phenomenology of two-Higgs-doublet models*. Phys. Rept. **516** (2012) 1–102, [arXiv:1106.0034](#) [hep-ph].
- [7] S. Hossenfelder and W. Hollik, *Two-loop corrections to the ρ parameter in Two-Higgs-Doublet Models*. Eur. Phys. J. C **77** (2017) no. 3, 178, [arXiv:1607.04610](#) [hep-ph].
- [8] S. Hossenfelder and W. Hollik, *Two-loop improved predictions for M_W and $\sin^2\theta_{\text{eff}}$ in Two-Higgs-Doublet models*. Eur. Phys. J. C **82** (2022) no. 10, 970, [arXiv:2207.03845](#) [hep-ph].
- [9] J. Braathen, M. D. Goodsell, and F. Staub, *Supersymmetric and non-supersymmetric models without catastrophic Goldstone bosons*. Eur. Phys. J. C **77** (2017) no. 11, 757, [arXiv:1706.05372](#) [hep-ph].
- [10] J. Braathen and S. Kanemura, *On two-loop corrections to the Higgs trilinear coupling in models with extended scalar sectors*. Phys. Lett. B **796** (2019) 38–46, [arXiv:1903.05417](#) [hep-ph].
- [11] J. Braathen and S. Kanemura, *Leading two-loop corrections to the Higgs boson self-couplings in models with extended scalar sectors*. Eur. Phys. J. C **80** (2020) no. 3, 227, [arXiv:1911.11507](#) [hep-ph].
- [12] G. Degrandi and P. Slavich, *On the two-loop BSM corrections to $h \rightarrow \gamma\gamma$ in the aligned THDM*. Eur. Phys. J. C **83** (2023) no. 10, 941, [arXiv:2307.02476](#) [hep-ph].
- [13] M. Aiko, J. Braathen, and S. Kanemura, *Leading two-loop corrections to the Higgs di-photon decay in the Inert Doublet Model*. [arXiv:2307.14976](#) [hep-ph].

- [14] D. A. Ross and M. J. G. Veltman, *Neutral Currents in Neutrino Experiments*. Nucl. Phys. B **95** (1975) 135–147.
- [15] G. Passarino, *The Interplay Between the Top Quark Mass and the Structure of the Higgs System*. Phys. Lett. B **231** (1989) 458–462.
- [16] B. W. Lynn and E. Nardi, *Radiative corrections in unconstrained $SU(2) \times U(1)$ and the top mass problem*. Nucl. Phys. B **381** (1992) 467–500.
- [17] T. Blank and W. Hollik, *Precision observables in $SU(2) \times U(1)$ models with an additional Higgs triplet*. Nucl. Phys. B **514** (1998) 113–134, [arXiv:hep-ph/9703392](#).
- [18] J. R. Forshaw, D. A. Ross, and B. E. White, *Higgs mass bounds in a triplet model*. JHEP **10** (2001) 007, [arXiv:hep-ph/0107232](#).
- [19] M.-C. Chen, S. Dawson, and T. Krupovnickas, *Constraining new models with precision electroweak data*. Int. J. Mod. Phys. A **21** (2006) 4045–4070, [arXiv:hep-ph/0504286](#).
- [20] M.-C. Chen, S. Dawson, and T. Krupovnickas, *Higgs triplets and limits from precision measurements*. Phys. Rev. D **74** (2006) 035001, [arXiv:hep-ph/0604102](#).
- [21] P. H. Chankowski, S. Pokorski, and J. Wagner, *(Non)decoupling of the Higgs triplet effects*. Eur. Phys. J. C **50** (2007) 919–933, [arXiv:hep-ph/0605302](#).
- [22] R. S. Chivukula, N. D. Christensen, and E. H. Simmons, *Low-energy effective theory, unitarity, and non-decoupling behavior in a model with heavy Higgs-triplet fields*. Phys. Rev. D **77** (2008) 035001, [arXiv:0712.0546 \[hep-ph\]](#).
- [23] M.-C. Chen, S. Dawson, and C. B. Jackson, *Higgs Triplets, Decoupling, and Precision Measurements*. Phys. Rev. D **78** (2008) 093001, [arXiv:0809.4185 \[hep-ph\]](#).
- [24] P. Fileviez Perez, H. H. Patel, M. J. Ramsey-Musolf, and K. Wang, *Triplet Scalars and Dark Matter at the LHC*. Phys. Rev. D **79** (2009) 055024, [arXiv:0811.3957 \[hep-ph\]](#).
- [25] L. Wang and X.-F. Han, *LHC diphoton and Z +photon Higgs signals in the Higgs triplet model with $Y = 0$* . JHEP **03** (2014) 010, [arXiv:1303.4490 \[hep-ph\]](#).
- [26] M. Chabab, M. C. Peyranère, and L. Rahili, *Probing the Higgs sector of $Y = 0$ Higgs Triplet Model at LHC*. Eur. Phys. J. C **78** (2018) no. 10, 873, [arXiv:1805.00286 \[hep-ph\]](#).
- [27] N. F. Bell, M. J. Dolan, L. S. Friedrich, M. J. Ramsey-Musolf, and R. R. Volkas, *Two-Step Electroweak Symmetry-Breaking: Theory Meets Experiment*. JHEP **05** (2020) 050, [arXiv:2001.05335 \[hep-ph\]](#).
- [28] C.-W. Chiang, G. Cottin, Y. Du, K. Fuyuto, and M. J. Ramsey-Musolf, *Collider Probes of Real Triplet Scalar Dark Matter*. JHEP **01** (2021) 198, [arXiv:2003.07867 \[hep-ph\]](#).
- [29] S. Ashanujjaman, S. Banik, G. Coloretti, A. Crivellin, B. Mellado, and A.-T. Mulaudzi, *$SU(2)_L$ triplet scalar as the origin of the 95 GeV excess?* Phys. Rev. D **108** (2023) no. 9, L091704, [arXiv:2306.15722 \[hep-ph\]](#).

- [30] J. Butterworth, H. Debnath, P. Fileviez Perez, and F. Mitchell, *Custodial symmetry breaking and Higgs boson signatures at the LHC*. Phys. Rev. D **109** (2024) no. 9, 095014, [arXiv:2309.10027 \[hep-ph\]](#).
- [31] S. Ashanujjaman, S. Banik, G. Coloretti, A. Crivellin, S. P. Maharathy, and B. Mellado, *Explaining the $\gamma\gamma + X$ Excesses at ≈ 151.5 GeV via the Drell-Yan Production of a Higgs Triplet*. [arXiv:2402.00101 \[hep-ph\]](#).
- [32] A. Crivellin, S. Ashanujjaman, S. Banik, G. Coloretti, S. P. Maharathy, and B. Mellado, *Growing Evidence for a Higgs Triplet*. [arXiv:2404.14492 \[hep-ph\]](#).
- [33] CDF Collaboration, T. Aaltonen *et al.*, *High-precision measurement of the W boson mass with the CDF II detector*. Science **376** (2022) no. 6589, 170–176.
- [34] ATLAS Collaboration, G. Aad *et al.*, *Measurement of the W -boson mass and width with the ATLAS detector using proton-proton collisions at $\sqrt{s} = 7$ TeV*. [arXiv:2403.15085 \[hep-ex\]](#).
- [35] CMS Collaboration, *Measurement of the W boson mass in proton-proton collisions at $\sqrt{s} = 13$ TeV*. CMS-PAS-SMP-23-002.
- [36] P. Fileviez Perez, H. H. Patel, and A. D. Plascencia, *On the W mass and new Higgs bosons*. Phys. Lett. B **833** (2022) 137371, [arXiv:2204.07144 \[hep-ph\]](#).
- [37] G. Senjanović and M. Zantedeschi, *$SU(5)$ grand unification and W -boson mass*. Phys. Lett. B **837** (2023) 137653, [arXiv:2205.05022 \[hep-ph\]](#).
- [38] M. A. Shifman, A. I. Vainshtein, M. B. Voloshin, and V. I. Zakharov, *Low-Energy Theorems for Higgs Boson Couplings to Photons*. Sov. J. Nucl. Phys. **30** (1979) 711–716.
- [39] B. A. Kniehl and M. Spira, *Low-energy theorems in Higgs physics*. Z. Phys. C **69** (1995) 77–88, [arXiv:hep-ph/9505225](#).
- [40] F. Staub, *SARAH*. [arXiv:0806.0538 \[hep-ph\]](#).
- [41] F. Staub, *From Superpotential to Model Files for FeynArts and CalcHep/CompHep*. Comput. Phys. Commun. **181** (2010) 1077–1086, [arXiv:0909.2863 \[hep-ph\]](#).
- [42] F. Staub, *Automatic Calculation of supersymmetric Renormalization Group Equations and Self Energies*. Comput. Phys. Commun. **182** (2011) 808–833, [arXiv:1002.0840 \[hep-ph\]](#).
- [43] F. Staub, *SARAH 3.2: Dirac Gauginos, UFO output, and more*. Comput. Phys. Commun. **184** (2013) 1792–1809, [arXiv:1207.0906 \[hep-ph\]](#).
- [44] F. Staub, *SARAH 4 : A tool for (not only SUSY) model builders*. Comput. Phys. Commun. **185** (2014) 1773–1790, [arXiv:1309.7223 \[hep-ph\]](#).
- [45] P. Chardonnet, P. Salati, and P. Fayet, *Heavy triplet neutrinos as a new dark matter option*. Nucl. Phys. B **394** (1993) 35–72.
- [46] K. Benakli, M. Goodsell, W. Ke, and P. Slavich, *W boson mass in minimal Dirac gaugino scenarios*. Eur. Phys. J. C **83** (2023) no. 1, 43, [arXiv:2208.05867 \[hep-ph\]](#).

- [47] M. Cirelli, N. Fornengo, and A. Strumia, *Minimal dark matter*. Nucl. Phys. B **753** (2006) 178–194, [arXiv:hep-ph/0512090](#).
- [48] N. Khan, *Exploring the hyperchargeless Higgs triplet model up to the Planck scale*. Eur. Phys. J. C **78** (2018) no. 4, 341, [arXiv:1610.03178 \[hep-ph\]](#).
- [49] J. R. Forshaw, A. Sabio Vera, and B. E. White, *Mass bounds in a model with a triplet Higgs*. JHEP **06** (2003) 059, [arXiv:hep-ph/0302256](#).
- [50] T. Hahn, *Generating Feynman diagrams and amplitudes with FeynArts 3*. Comput. Phys. Commun. **140** (2001) 418–431, [arXiv:hep-ph/0012260](#).
- [51] A. I. Davydychev and J. B. Tausk, *Two loop selfenergy diagrams with different masses and the momentum expansion*. Nucl. Phys. B **397** (1993) 123–142.
- [52] H.-Q. Zheng and D.-D. Wu, *First order QCD corrections to the decay of the Higgs boson into two photons*. Phys. Rev. D **42** (1990) 3760–3763.
- [53] A. Djouadi, M. Spira, J. J. van der Bij, and P. M. Zerwas, *QCD corrections to $\gamma\gamma$ decays of Higgs particles in the intermediate mass range*. Phys. Lett. B **257** (1991) 187–190.
- [54] S. Dawson and R. P. Kauffman, *QCD corrections to $H \rightarrow \gamma\gamma$* . Phys. Rev. D **47** (1993) 1264–1267.
- [55] K. Melnikov and O. I. Yakovlev, *Higgs \rightarrow two photon decay: QCD radiative correction*. Phys. Lett. B **312** (1993) 179–183, [arXiv:hep-ph/9302281](#).
- [56] A. Djouadi, M. Spira, and P. M. Zerwas, *Two photon decay widths of Higgs particles*. Phys. Lett. B **311** (1993) 255–260, [arXiv:hep-ph/9305335](#).
- [57] M. Inoue, R. Najima, T. Oka, and J. Saito, *QCD corrections to two photon decay of the Higgs boson and its reverse process*. Mod. Phys. Lett. A **9** (1994) 1189–1194.
- [58] J. Fleischer, O. V. Tarasov, and V. O. Tarasov, *Analytical result for the two loop QCD correction to the decay $H \rightarrow 2$ gamma*. Phys. Lett. B **584** (2004) 294–297, [arXiv:hep-ph/0401090](#).
- [59] Y. Liao and X.-y. Li, *$O(\alpha^{**2} G(F)m(t)**2)$ contributions to $H \rightarrow \gamma\gamma$* . Phys. Lett. B **396** (1997) 225–230, [arXiv:hep-ph/9605310](#).
- [60] A. Djouadi, P. Gambino, and B. A. Kniehl, *Two loop electroweak heavy fermion corrections to Higgs boson production and decay*. Nucl. Phys. B **523** (1998) 17–39, [arXiv:hep-ph/9712330](#).
- [61] F. Fugel, B. A. Kniehl, and M. Steinhauser, *Two loop electroweak correction of $O(G(F)M(t)**2)$ to the Higgs-boson decay into photons*. Nucl. Phys. B **702** (2004) 333–345, [arXiv:hep-ph/0405232](#).
- [62] G. Degrandi and F. Maltoni, *Two-loop electroweak corrections to the Higgs-boson decay $H \rightarrow \gamma\gamma$* . Nucl. Phys. B **724** (2005) 183–196, [arXiv:hep-ph/0504137](#).
- [63] U. Aglietti, R. Bonciani, G. Degrandi, and A. Vicini, *Two loop light fermion contribution to Higgs production and decays*. Phys. Lett. B **595** (2004) 432–441, [arXiv:hep-ph/0404071](#).

- [64] U. Aglietti, R. Bonciani, G. Degrossi, and A. Vicini, *Master integrals for the two-loop light fermion contributions to $gg \rightarrow H$ and $H \rightarrow \gamma\gamma$* . Phys. Lett. B **600** (2004) 57–64, [arXiv:hep-ph/0407162](#).
- [65] G. Passarino, C. Sturm, and S. Uccirati, *Complete Two-Loop Corrections to $H \rightarrow \gamma\gamma$* . Phys. Lett. B **655** (2007) 298–306, [arXiv:0707.1401](#) [hep-ph].
- [66] S. Actis, G. Passarino, C. Sturm, and S. Uccirati, *NNLO Computational Techniques: The Cases $H \rightarrow \gamma\gamma$ and $H \rightarrow g g$* . Nucl. Phys. B **811** (2009) 182–273, [arXiv:0809.3667](#) [hep-ph].
- [67] **CMS** Collaboration, A. Tumasyan *et al.*, *A portrait of the Higgs boson by the CMS experiment ten years after the discovery*. Nature **607** (2022) no. 7917, 60–68, [arXiv:2207.00043](#) [hep-ex].
- [68] M. Cepeda *et al.*, *Report from Working Group 2: Higgs Physics at the HL-LHC and HE-LHC*. CERN Yellow Rep. Monogr. **7** (2019) 221–584, [arXiv:1902.00134](#) [hep-ph].
- [69] J. Braathen and M. D. Goodsell, *Avoiding the Goldstone Boson Catastrophe in general renormalisable field theories at two loops*. JHEP **12** (2016) 056, [arXiv:1609.06977](#) [hep-ph].
- [70] J. Braathen, M. D. Goodsell, and P. Slavich, *Matching renormalisable couplings: simple schemes and a plot*. Eur. Phys. J. C **79** (2019) no. 8, 669, [arXiv:1810.09388](#) [hep-ph].